1/*N* expansion in the vibron model: Diatomic molecules

S. Kuyucak* and M. K. Roberts
Department of Theoretical Physics, Research School of Physical Sciences, Australian National University, Canberra, Australian Capital Territory 0200, Australia
(Received 13 November 1997)

Using angular-momentum-projected mean-field theory, we develop 1/*N* expansion solutions for the vibron model of diatomic molecules. Analytic expressions of spectroscopic accuracy are derived for rotational-vibrational energy levels and for the intensities of transitions among them. The results are used in a systematic study of diatomic molecules in the vibron model with a view to finding appropriate Hamiltonians for a realistic description of rotation-vibration spectra. [S1050-2947(98)00905-6]

PACS number(s): 33.20.−t, 31.15.Hz

I. INTRODUCTION

Algebraic techniques, and especially-spectrum generating algebras (SGA's), have been playing an increasingly important role in the treatment of various quantum-mechanical systems. The interacting boson model (IBM) [1], in particular, has made a large impact in nuclear structure studies during the last two decades. The vibron model [2,3] provides a similar algebraic framework for treating problems in molecular spectroscopy. It has been especially useful in describing complex spectra of polyatomic molecules where traditional methods based on solving the Schrödinger equation in coordinate space run into difficulties. The algebraic techniques developed in the nuclear case can be readily applied to the vibron model and could play a similarly rejuvenating role in molecular spectroscopy.

The basic building blocks of the vibron model are the scalar s and vector p bosons. The latter represents the dipole degree of freedom in a molecular bond while the former is needed to generate a finite, anharmonic, spectrum. The 16 bilinear operators $\{b^{\dagger}_{lm}b_{lm},\ l=0,1,\ m=-l,\ldots,l\}$ close under the U(4) algebra which forms the backbone of the model (here we use the notation $b_{00}=s$, $b_{1m}=p_m$). The U(4) algebra has two rotationally invariant subalgebra chains, namely, (i) U(4)⊃U(3)⊃O(3)⊃O(2) and (ii) U(4)⊃O(4)⊃O(3)⊃O(2). When the Hamiltonian describing the boson system is written in terms of the Casimir operators in one of the chains, the eigenvalue problem can be solved analytically. In this way, complete solutions for the U(3) and O(4) dynamical symmetry limits have been obtained [2,3]. The U(3) limit leads to a vibrational spectrum and is not of much relevance to molecules. The O(4) limit, on the other hand, leads to a spectrum similar to that of a Morse potential and hence it is appropriate for the description of the rotation-vibration spectra of molecules.

In its simplest form with a one-body dipole operator, the O(4) limit corresponds to a rigid rotor with vanishing vibrational transitions, and so it does not give a very accurate representation of the data. This zeroth-order description can be improved in two ways. The first, which has been exclusively used in the literature so far, is to preserve the O(4) symmetry by adding higher-order Casimir operators to the Hamiltonian. The one-body transition operator is extended similarly by including many-body terms. Although this approach has the advantage that analytic expressions for energies (like the Dunham expansion) and transitions can be readily given, this comes at the cost of introducing many more parameters in the model. In the second method, one breaks the O(4) symmetry by adding terms from the U(3) chain to the Hamiltonian. A general study of symmetry-breaking effects requires numerical diagonalization of the Hamiltonian, which may explain why it has been neglected. In contrast, symmetry breaking has been the main approach in realistic applications of the IBM to collective nuclei [1]. While the degree of symmetry breaking is much larger in the IBM, making its study almost unavoidable, a similar approach may lead to a more economical description of spectroscopic data in the vibron model, and therefore it would be worthwhile to investigate it in some detail.

The angular-momentum-projected mean-field theory provides analytic solutions for SGA's in the form of a 1/*N* expansion [4]. Thus it avoids the drudgery of numerical diagonalization and could facilitate a systematic study of symmetry-breaking effects in the vibron model. The 1/*N* expansion method has previously been applied to various nuclear structure and reaction problems (see [5] for a recent review), where it played a useful role both conceptually and as a computational tool. The purpose of this paper is to develop the 1/*N* expansion technique for the vibron model of diatomic molecules. Analytic expressions are derived for energy levels and electromagnetic transitions, which are then used in a systematic study of the symmetry breaking to assess whether it provides a viable alternative to the symmetry-preserving approach.

A unique feature of the U(4) algebra is that it provides the simplest, nontrivial SGA's that can be solved exactly using the 1/*N* expansion method. This is possible because diatomic molecules possess axial symmetry in the intrinsic frame, which simplifies the formalism and allows evaluation of the projection integrals in closed form. [In the IBM, except in the SU(3) limit, axial symmetry is realized only approximately; hence the solutions are not exact at higher orders.] In this sense, the 1/*N* expansion in the vibron model could play

*Electronic address: sek105@rsphysse.anu.edu.au

a similar role as the Lipkin model [6], which has been widely used in testing various many-body techniques. Because the vibron model is formulated in three dimensions instead of one, it can also be used in checking the accuracy of approximate angular momentum projection methods such as cranking.

Finally, the U(4) SGA of diatomic molecules forms the basis for extensions of the vibron model to polyatomic molecules. A clear understanding of a single molecular bond in the vibron model is necessary before the $1/N$ expansion technique can be applied to more complex molecules. A brief version of this work has already appeared in Ref. [7]. Extensions to polyatomic molecules and collision processes will be pursued in future articles.

II. FORMALISM

In this section, we introduce vibron model Hamiltonians for diatomic molecules that generalize the dynamical symmetry limits. We briefly discuss the formulation of the mean-field theory in the intrinsic frame and then present the angular momentum projection technique that leads to the $1/N$ expansion formalism. The section ends with the construction of the projected vibrational states in the laboratory frame.

A. Hamiltonian and transition operators

The Hamiltonians in the O(4) and U(3) symmetry limits of the vibron model can be written in the multipole form as [2]

$$\hat{H}_{\mathrm{O}(4)} = -\kappa \hat{D}\cdot\hat{D} + \kappa' \hat{L}\cdot\hat{L},$$

$$\hat{H}_{\mathrm{U}(3)} = \varepsilon \hat{n}_p + \sigma \hat{n}_p^2 + \kappa' \hat{L}\cdot\hat{L}. \tag{2.1}$$

Here κ, κ', ε, and σ are the model parameters that are determined from fits to spectra. The dipole, angular momentum, and the p-boson number operators in Eqs. (2.1) are defined by

$$\hat{D}_\mu = [s^\dagger \tilde{p} + p^\dagger \tilde{s}]^{(1)}_\mu,$$

$$\hat{L}_\mu = -\sqrt{2}[p^\dagger \tilde{p}]^{(1)}_\mu,$$

$$\hat{n}_p = \sum_\mu p^\dagger_\mu p_\mu, \tag{2.2}$$

where brackets denote tensor coupling and the tilde, $\tilde{b}_{lm} = (-1)^m b_{l-m}$, ensures that the boson annihilation operators transform like spherical tensors. Combining all the terms in Eqs. (2.1), one obtains the most general Hamiltonian with one- and two-body interactions:

$$\hat{H} = -\kappa \hat{D}\cdot\hat{D} + \kappa' \hat{L}\cdot\hat{L} + \varepsilon \hat{n}_p + \sigma \hat{n}_p^2. \tag{2.3}$$

We have excluded a constant term from Eq. (2.3), as our main interest is in the excitation spectrum. There are various other forms of the vibron model Hamiltonian but they can all be shown to be equivalent to Eq. (2.3) up to a constant.

Although the main focus of this paper is to study the symmetry breaking envisaged by the Hamiltonian (2.3), higher-order interactions may be useful in refinements of the model. Therefore, we will also consider the effect of three-body terms on the spectrum. In general, there are eight independent three-body terms that one can write down [9]. However, most of these are either constant or can be absorbed in the one- and two-body parts of the Hamiltonian. Only three of them make genuine three-body contributions to the excitation spectrum, and they can be constructed from the operators in Eqs. (2.2) as

$$\hat{H}_3 = \tau_1 \hat{n}_p^3 + \tau_2(\hat{n}_p \hat{D}^2 + \hat{D}^2 \hat{n}_p) + \tau_3 \hat{n}_p \hat{L}^2, \tag{2.4}$$

where τ_i are parameters that determine the strength of the interactions. The middle term in Eq. (2.4) has been symmetrized because the two operators do not commute and $\hat{H}_3$ would not be Hermitian otherwise.

To calculate various electromagnetic transitions among molecular levels, one needs the appropriate transition operators in the vibron model. For infrared transitions, the dipole operator introduced in Eqs. (2.2) provides a lowest-order approximation. A more refined description of vibrational transitions requires inclusion of higher-order terms in the transition operator [2]

$$\hat{T}^{(1)}_\mu = d_0 \hat{D}_\mu + d_1(\hat{n}_p \hat{D}_\mu + \hat{D}_\mu \hat{n}_p) + d_2(\hat{n}_p^2 \hat{D}_\mu + \hat{D}_\mu \hat{n}_p^2) + \cdots. \tag{2.5}$$

In this work, we limit ourselves to the calculation of the first two terms in Eq. (2.5), which is sufficient for a description of dipole transitions among the first few vibrational bands. We will see that Eq. (2.5) is not adequate for transitions involving higher-vibrational bands, and a generalization of Eq. (2.5) to an exponential form given by

$$\hat{T}^{(1)}_\mu = d_0 \hat{D}_\mu + d_1(e^{\lambda \hat{n}_p} \hat{D}_\mu + \hat{D}_\mu e^{\lambda \hat{n}_p}) \tag{2.6}$$

is necessary [8]. Matrix elements of the operator (2.6) are difficult to evaluate with projection, and therefore will not be considered here. Nevertheless, these have been evaluated using mean-field theory [8] and are sufficient for practical purposes.

For Raman transitions, one needs tensor operators of rank 0 and 2. To lowest order, these are given by

$$\hat{T}^{(0)}_0 = \alpha_0 \hat{n}_p, \quad \hat{T}^{(2)}_\mu = \alpha_2 \hat{Q}_\mu, \tag{2.7}$$

where the quadrupole operator is defined as

$$\hat{Q}_\mu = [p^\dagger \tilde{p}]^{(2)}_\mu. \tag{2.8}$$

B. Mean-field theory

Mean-field techniques have been extensively used in the vibron model to discuss its geometrical content and to provide a link with the more conventional models based on geometrical variables [9–15]. Since the number of bosons, N, is conserved in the vibron model, the variational state used in the mean-field calculations is a projective coherent state or, in more descriptive terms, a simple condensate of N intrinsic bosons. Exploiting the axial symmetry of diatomic molecules, one can choose the molecular axis along the z direction so that the variational state for the ground band of the system can be written as

$$|N,r\rangle=(N!)^{-1/2}(b^{\dagger})^{N}|0\rangle, \quad b^{\dagger}=(1+r^2)^{-1/2}(s^{\dagger}+rp_0^{\dagger}). \tag{2.9}$$

Here $b^{\dagger}$ denotes the intrinsic boson operator and r is a variational parameter. The variable r is related to the interatomic distance in the classical limit of the vibron model ($N\rightarrow\infty$), but the functional form of this relationship appears to be exponential rather than linear [11,15]. For a given Hamiltonian $\hat{H}$, r is determined from the energy surface

$$E(r)=\langle N,r|\hat{H}|N,r\rangle \tag{2.10}$$

by a variational procedure. For the Hamiltonian (2.3), the energy surface is given by

$$E(r)=\frac{Nr^2}{1+r^2}\left[-\kappa\left(\frac{4(N-1)}{1+r^2}+\frac{3+r^2}{r^2}\right)+2\kappa'+\varepsilon+\sigma\left(\frac{(N-1)r^2}{1+r^2}+1\right)\right]. \tag{2.11}$$

Variation of Eq. (2.11) will be discussed in the next section after we compare it with the projected ground-band energies.

Vibrational bands, denoted by $|N,v\rangle$, can be obtained from Eqs. (2.9) by replacing the intrinsic bosons b with the orthogonal fluctuation bosons b':

$$|N,v\rangle=[(N-v)!v!]^{-1/2}(b^{\dagger})^{N-v}(b'^{\dagger})^{v}|0\rangle,$$

$$b'^{\dagger}=[1+r^2]^{-1/2}(rs^{\dagger}-p_0^{\dagger}), \tag{2.12}$$

where v is the vibrational quantum number. These bands are orthogonal by construction, that is, $\langle N,v|N,v'\rangle=\delta_{v,v'}$. Energy expressions for the vibrational bands follow from the expectation value of $\hat{H}$ in the states (2.12):

$$E_v=\langle N,v|\hat{H}|N,v\rangle. \tag{2.13}$$

Note that r is already fixed from the ground band, and therefore it does not appear in the vibrational energies as a variable. Thus variation of the energy surface (2.10), in effect, determines the whole spectrum. The vibrational band excitation energies for the Hamiltonian (2.3) are obtained by subtracting the ground energy (2.11) from (2.13), and given by

$$E_v-E_0=v(1+r^2)^{-2}\{2\kappa(N-v)[8r^2-(1-r^2)^2]+\sigma[2N(2-r^2)r^2+v(r^4-4r^2+1)]+(2\kappa+2\kappa'+\varepsilon)(1-r^4)\}. \tag{2.14}$$

One can also use the states (2.12) to discuss electromagnetic transitions among vibrational bands. For the lowest-order dipole operator in Eq. (2.5), the only nonzero matrix elements are between the states v and $v'=v$, $v\pm1$:

$$\langle N,v|\hat{D}_0|N,v\rangle=(N-2v)2r/(1+r^2), \tag{2.15}$$

$$\langle N,v|\hat{D}_0|N,v+1\rangle=[(N-v)(v+1)]^{1/2}(r^2-1)/(1+r^2). \tag{2.16}$$

Note that Eq. (2.16) vanishes in the O(4) limit ($r=1$) but not in general. This provides a first glimpse of how breaking of the O(4) symmetry may lead to an improved agreement with data.

C. Angular momentum projection

Because the condensate states (2.12) break the rotational invariance, matrix elements obtained in the intrinsic frame are correct to leading order in $1/N$ [4]. Hence the mean-field theory provides only an approximate solution, suitable for a qualitative description of spectroscopic quantities. For comparison with experimental data, one needs more accurate results, which can be achieved by performing angular momentum projection before variation. Since variation after projection (VAP) with a complete set of states is equivalent to solving the Schrödinger equation, this approach can provide analytical solutions for general vibron model Hamiltonians. Such a program has been carried out in the IBM [4] and was shown to lead to a $1/N$ expansion for all matrix elements.

Angular momentum projection from a general intrinsic state is rather complicated and usually requires a large numerical effort [16]. The situation is considerably simplified if the system has axial symmetry. Then the intrinsic states have well-defined quantum numbers K for projection on to the body-fixed axis, and the expectation value of a Hamiltonian in an intrinsic state ϕ_K is given by

$$E(L)=\langle\phi_K|HP^L_{KK}|\phi\rangle/\langle\phi|P^L_{KK}|\phi_K\rangle, \tag{2.17}$$

where P^L_{MK} is the projection operator defined as [17]

$$P^L_{MK}=\frac{2L+1}{8\pi^2}\int D^{L*}_{MK}(\Omega)R(\Omega)d\Omega. \tag{2.18}$$

In Eq. (2.18), $R(\Omega)$ is the rotation operator which rotates the system through the three Euler angles (α,β,γ), collectively denoted by Ω, and D^L_{MK} is a Wigner D function. Note that in Eq. (2.17) the expectation value is divided by the normalization because, contrary to Eq. (2.10), the projected states are not normalized. Since all the intrinsic states (2.12) have $K=0$, the α and γ integrals in Eq. (2.18) simply give 2π each, and the projection operator takes a particularly simple form

$$P^L_{00}=\frac{2L+1}{2}\int_0^{\pi}d\beta\ \sin\beta P_L(\cos\beta)e^{-i\beta\hat{L}_y}. \tag{2.19}$$

Here we have used $D^{L*}_{00}(\Omega)=P_L(\cos\beta)$, which is a Legendre function, and $\hat{L}_y$ is the y component of the angular momentum operator $\hat{L}$.

As an illustration of how the $1/N$ expansion follows from angular momentum projection, we evaluate the normalization $\mathcal{N}(N,L)$ for the condensate (2.9) in some detail. As will be seen later, all the matrix elements can be reduced to expressions containing $\mathcal{N}(N,L)$; therefore their accuracy depends directly on how accurately $\mathcal{N}(N,L)$ is evaluated. Besides the key role it plays in the formulation of the method, $\mathcal{N}(N,L)$ also serves as a simple example to demonstrate the boson calculus and angular momentum algebra techniques,

which are extensively used in the $1/N$ expansion calculations. From Eq. (2.19), $\mathcal{N}(N,L)$ is defined as

$$\mathcal{N}(N,L)=\langle N,r|P^L_{00}|N,r\rangle,$$
$$=\frac{2L+1}{2N!}\int_0^\pi d\beta\ \sin\beta\ P_L(\cos\beta)$$
$$\times\langle 0|b^N e^{-i\beta\hat{L}_y}(b^\dagger)^N|0\rangle. \tag{2.20}$$

The first step is to apply a rotation operator to the condensate. Writing the condensate explicitly as a product and inserting the identity operator $I=e^{-i\beta\hat{L}_y}e^{i\beta\hat{L}_y}$ in between each product, it is clear that rotating the condensate is equivalent to a condensate of rotated intrinsic bosons $b^\dagger_R$ defined as

$$b^\dagger_R=e^{-i\beta\hat{L}_y}b^\dagger e^{i\beta\hat{L}_y}. \tag{2.21}$$

Using the well-known formula for the rotation of spherical tensors [17], we obtain from Eq. (2.21)

$$b^\dagger_R=(1+r^2)^{-1/2}\left(s^\dagger+r\sum_m\ d^1_{m0}(\beta)p^\dagger_m\right), \tag{2.22}$$

where d^1_{m0} is a Wigner d function. The next step is to evaluate the matrix element in Eq. (2.20). The standard technique is to commute all the annihilation operators to the right, which could be cumbersome especially in cases involving many different (but not commuting) boson operators. Schwinger's boson calculus [18], where one replaces the annihilation operators by differentials acting on the creation operators (or vice versa), offers a much simpler method for this purpose. Thus the matrix element in Eq. (2.20) can be written as

$$\langle 0|b^N(b^\dagger_R)^N|0\rangle=\langle 0|(\partial/\partial b^\dagger)^N(b^\dagger_R)^N|0\rangle$$
$$=N!\langle 0|(\partial b^\dagger_R/\partial b^\dagger)^N|0\rangle. \tag{2.23}$$

The last derivative corresponds to a simple contraction of two boson operators; e.g., for $b=\Sigma_i x_i b_i$, $b'=\Sigma_j x'_j b_j$, it is given by

$$\langle 0|bb'^\dagger|0\rangle=\langle 0|\partial b'^\dagger/\partial b^\dagger|0\rangle=\left\langle 0\left|\sum_{ij}\ x_i x'_j(\partial b^\dagger_j/\partial b^\dagger_i)\right|0\right\rangle$$
$$=\sum_{ij}\ x_i x'_j\,\delta_{ij}=\sum_i\ x_i x'_i\,. \tag{2.24}$$

Using this result in Eqs. (2.22) and (2.23), we obtain for the matrix element

$$\langle 0|b^N(b^\dagger_R)^N|0\rangle=N!\left[\frac{1+r^2\cos\beta}{1+r^2}\right]^N\equiv N![Z(\beta)]^N. \tag{2.25}$$

Substituting Eq. (2.25) in Eq. (2.20), yields the following integral for the normalization:

$$\mathcal{N}(N,L)=\frac{2L+1}{2}\int_0^\pi d\beta\ \sin\beta\ P_L(\cos\beta)[Z(\beta)]^N. \tag{2.26}$$

After the transformation $z=\cos\beta$, the integral in Eq. (2.26) takes the form

$$\mathcal{N}(N,L)=\frac{2L+1}{2(1+r^2)^N}\int_{-1}^1 dz P_L(z)[1+r^2z]^N. \tag{2.27}$$

Although it looks deceptively simple, this integral is not available in standard tables, and only recently has it been evaluated in closed form in terms of the hypergeometric function ${}_2F_1$ [19]. We refer to Ref. [19] for details of the integration and simply quote the final result here:

$$\mathcal{N}(N,L)=\left(\frac{2L+1}{N+1}\right)\left(\frac{1+r^2}{2r^2}\right)\Bigg[{}_2F_1(-L,L+1;N+2;(1+r^2)/2r^2)-(-1)^L\left(\frac{1-r^2}{1+r^2}\right)^{N+1}_2F_1(-L,L+1;N+2;(-1+r^2)/2r^2)\Bigg]. \tag{2.28}$$

Here the first term arises from the integral range $[1,0]$ and the second one from $[0,-1]$. For identical-parity boson systems, the second term would be equal to the first one, leading to a factor of 2. For the mixed-parity sp-boson system, the second term is clearly much smaller than the first one, suppressed by the exponential factor in front. In fact, it vanishes in the O(4) limit when $r=1$, and it is completely negligible for realistic breaking of the O(4) limit when r is near 1 (in a typical case with $r=1.2$, $N=40$, the suppression factor is 10^{-30}). Therefore, in the following, we will ignore the contributions from the second term to simplify the expressions.

To make further progress, we first note that the quantity a, defined as

$$a=2r^2/(1+r^2), \tag{2.29}$$

provides a more convenient parametrization for $\mathcal{N}(N,L)$. Since the mapping is one to one ($[0,\infty]$ is mapped onto $[0,2]$) and monotonous, it will have no effect on the variational problem. This choice for a is preferred over its inverse, because physically it corresponds to the ''average angular momentum squared'' carried by an intrinsic boson. To bring $\mathcal{N}(N,L)$ into a standard form, we write the hypergeometric function in Eq. (2.28) explicitly as

$${}_2F_1(-L,L+1;N+2;x)=1-\frac{\bar{L}}{N+2}x+\frac{\bar{L}(\bar{L}-2)}{2(N+2)(N+3)}x^2-\frac{\bar{L}(\bar{L}-2)(\bar{L}-6)}{3!(N+2)(N+3)(N+4)}x^3+\cdots. \tag{2.30}$$

Here the overbar denotes the angular momentum eigenvalues, $\bar{L}\equiv L(L+1)$. Since projection involves $\bar{L}$ rather than L, we will use this compact notation throughout the paper. Expanding Eq. (2.30) in $1/N$ and $\bar{L}$ finally yields the desired $1/N$ expansion for the normalization:

$$\mathcal{N}(N,L)=\frac{2L+1}{aN}\Bigg[1-\frac{1}{aN}(\overline{L}+a)+\frac{1}{2(aN)^2}[\overline{L^2}+(6a-2)\overline{L}+2a^2]-\frac{1}{3!(aN)^3}[\overline{L^3}+(18a-8)\overline{L^2}+(42a^2-36a+12)\overline{L}+6a^3]+\ldots\Bigg]. \tag{2.31}$$

Note that the expansion is in fact in the product aN, which corresponds to the ''average angular momentum squared'' of the condensate [20]. While it may seem more appealing to use $L_c=aN$ rather than N itself as the expansion parameter, we refrain from doing so because N is a fixed number whereas a is a variational parameter dependent on the choice of the Hamiltonian.

For future notational convenience, we introduce a reduced normalization function $F(N,L)=\mathcal{N}(N,L)/(2L+1)$, and rewrite Eq. (2.31) in a compact form

$$F(N,L)=\frac{1}{aN}\sum_{n=0}\frac{(-1)^n}{n!(aN)^n}\sum_{m=0}^{n}\alpha_{nm}\overline{L}^m. \tag{2.32}$$

As is seen from Eq. (2.31), the coefficients α_{nm} are polynomials in a. A complete list to order $1/N^6$ is given in Appendix A. As a general terminology, the leading coefficients in each power of $1/N$, α_{nn}, are called first layer, the second ones, α_{nn-1}, second layer, etc. The significance of the concept of layers will be apparent when we evaluate matrix elements in the next section. Finally, we note that the second term in Eq. (2.28) leads to an identical expansion in $1/N$ and $\overline{L}$. Thus, should the need arise, it could be easily included in the final result by modifying the coefficients α_{nm}.

D. Construction of projected states

The condensate (2.9), with the VAP procedure, provides an exact description of the ground-band ($v=0$) states. The same thing is not true for the vibrational bands (2.12) defined in the intrinsic frame. First, although they are orthogonal by construction, this property is lost after angular momentum projection. Second, comparison with the exact form of the states in the O(4) limit [see Eq. (B6) in Appendix B] shows that there are extra pieces involved. We use the O(4) limit as a guide in constructing a new set of vibrational states in the intrinsic frame, which remain orthogonal after projection. Inspecting the O(4) intrinsic states in Eq. (B6) suggests the form

$$|N,v=1\rangle=[(N-1)!]^{-1/2}[b^\dagger b'^\dagger+\xi_1 p_1^\dagger p_{-1}^\dagger](b^\dagger)^{N-2}|0\rangle,$$

$$|N,v=2\rangle=[2!(N-2)!]^{-1/2}[(b^\dagger)^2(b'^\dagger)^2-2\xi_2 b^\dagger b'^\dagger p_1^\dagger p_{-1}^\dagger+\xi_2'(p_1^\dagger p_{-1}^\dagger)^2](b^\dagger)^{N-4}|0\rangle. \tag{2.33}$$

We limit ourselves to the first two vibrational bands in this work, but it should be obvious from these examples how to construct intrinsic states for higher-vibrational bands. In Eq. (2.33), the coefficients ξ are determined from orthogonality conditions with the lower-vibrational bands. For example, orthogonality of the $v=0$ and $v=1$ bands requires

$$\langle N,v=1|P_{00}^L|N,v=0\rangle=0, \tag{2.34}$$

which, after some boson calculus, translates to the condition

$$\int_0^\pi d\beta\ \sin\beta\ d_{00}^L\{[Z(\beta)]^{N-1}r(1-d_{00}^1)+\xi_1[Z(\beta)]^{N-1}r^2 d_{10}^1 d_{-10}^1\}=0, \tag{2.35}$$

where $Z(\beta)$ is defined in Eq. (2.25). Using Eq. (C1), one can couple the various d functions in Eq. (2.35) to a single function d_{00}^J. The resulting β integral has the same form as the normalization integral in Eq. (2.26), and hence the condition (2.35) can be written as

$$\sum_J\Bigg[\sum_{l=0}^{1}(-1)^l F(N-1,J)+\xi_1 r\sum_l\langle 11\ \ 1-1|l0\rangle\times\langle 10\ \ 10|l0\rangle F(N-2,J)\Bigg]\langle L0\ \ l0|J0\rangle^2=0. \tag{2.36}$$

We refer to Appendix C for evaluation of the angular momentum sums over the Clebsch-Gordan (CG) coefficients in Eq. (2.36). Both these sums and the division in Eq. (2.36) can be carried out most efficiently using the MATHEMATICA software [21]. The resulting expression for ξ_1 to order $1/N^5$ is given by

$$\xi_1=\left(\frac{2-a}{a}\right)^{1/2}\Bigg\{1+\frac{2(1-a)}{aN}\sum_{m=0}\left(\frac{2-a}{aN}\right)^m-\frac{\overline{L}}{(aN)^2}2(1-a)\Bigg[1+\frac{7-5a}{aN}+\frac{3(2-a)(6-5a)}{(aN)^2}+\frac{176-336a+201a^2-37a^3}{(aN)^3}\Bigg]-\frac{\overline{L^2}}{(aN)^3}(1-a)\times\Bigg[1+\frac{2}{aN}-\frac{3(12-24a+11a^2)}{(aN)^2}\Bigg]-\frac{\overline{L^3}}{(aN)^4}(1-a)\Bigg[1+\frac{2(2-a)}{aN}\Bigg]-\frac{\overline{L^4}}{(aN)^5}(1-a)\Bigg\}, \tag{2.37}$$

where we have substituted $r=[a/(2-a)]^{1/2}$ from Eq. (2.29). Orthogonality of the $v=2$ band to the $v=0$ and 1 bands requires

$$\langle N,v=2|P_{00}^L|N,v=0\rangle=0,\quad \langle N,v=2|P_{00}^L|N,v=1\rangle=0. \tag{2.38}$$

Following steps similar to above, the two conditions in Eq. (2.38) can be converted to two linear equations in the unknowns ξ_2 and ξ_2'. These, in turn, can be easily solved for each power of $\overline{L}$ and $1/N$, leading to the expressions (to order $1/N^4$)

$$\xi_2=\left(\frac{2-a}{a}\right)^{1/2}\left\{1+\frac{2(1-a)}{aN}\sum_{m=0}\left(\frac{4-a}{aN}\right)^m-\frac{\overline{L}}{(aN)^2}2(1-a)\right.$$
$$\times\left[1+\frac{11-5a}{aN}+\frac{3(34-32a+7a^2)}{(aN)^2}\right]$$
$$\left.-\frac{\overline{L^2}}{(aN)^3}(1-a)\left[1+\frac{8}{aN}\right]-\frac{\overline{L^3}}{(aN)^4}(1-a)\right\},$$

$$\xi_2'=\left(\frac{2-a}{a}\right)\left\{1+\frac{4(1-a)}{aN}\sum_{m=0}\left(\frac{4-a}{aN}\right)^m-\frac{\overline{L}}{(aN)^2}4(1-a)\right.$$
$$\times\left[1+\frac{11-5a}{aN}+\frac{3(4-a)(8-5a)}{(aN)^2}\right]$$
$$\left.-\frac{\overline{L^2}}{(aN)^3}2(1-a)\left[1+\frac{2+6a}{aN}\right]-\frac{\overline{L^3}}{(aN)^4}2(1-a)\right\}. \tag{2.39}$$

The O(4) limit ($r=a=1$) provides a useful check against any errors in the calculations. For $a=1$, all the coefficients ξ in Eqs. (2.37) and (2.39) reduce to 1 in agreement with the group theoretical result given in Eq. (B6).

As in the case of the ground band, the vibrational intrinsic states (2.33) need to be normalized in the laboratory frame. The normalization for the state $|N,v\rangle$ is defined as

$$\mathcal{N}(N,v,L)=\langle N,v|P^L_{00}|N,v\rangle. \tag{2.40}$$

Evaluation of these matrix elements is similar to the cases discussed above but much longer due to the extra terms (e.g., for $v=1$, there are seven distinct terms in the normalization). Since there is not much to be gained from these exercises in the use of MATHEMATICA, we prefer not to go into any details, but simply list the resulting normalization coefficients for the $v=1$ and 2 bands in Appendix A.

III. ENERGIES

Molecular energy levels are very accurately measured, and to match that accuracy in calculations, one needs to develop the $1/N$ expansion to fairly high orders. While this is not a serious problem owing to the recent developments in computer algebra, one would still like to avoid unwieldy expressions which have little information content. In this section, we first show how the layer structure in the $1/N$ expansion fulfills this role by tailoring the expressions to the required accuracy with maximum efficiency in algebraic manipulations. In the following subsections, we derive energy formulas for the ground band and discuss the ensuing variational problem. Energy formulas for the first two vibrational bands are presented at the end.

A. General form

The general form of the $1/N$ expansion for energy levels has been conjectured in previous work [4] but not proved explicitly. Here we demonstrate the layer structure inherent in the $1/N$ expansion with an explicit calculation of one-body energies. The expectation value of a general one-body operator $\hat{n}_l=\Sigma_m b^\dagger_{lm}b_{lm}$, with angular momentum projection, is given by

$$\langle\hat{n}_l\rangle_L=\langle N,r|\hat{n}_l P^L_{00}|N,r\rangle/\mathcal{N}(N,L), \tag{3.1}$$

where $\mathcal{N}(N,L)$ is the normalization. Following steps similar to Sec. II C and introducing $F(N,L)$ from Eq. (2.32), this can be written as

$$\langle\hat{n}_l\rangle_L=\frac{1}{2N!F(N,L)}\int d\beta(\sin\beta)d^L_{00}(\beta)\langle 0|b^N\hat{n}_l(b^\dagger_R)^N|0\rangle. \tag{3.2}$$

The matrix element in Eq. (3.2) can be evaluated using boson calculus:

$$\langle 0|b^N\hat{n}_l(b^\dagger_R)^N|0\rangle=N!N\left(\frac{\partial b^\dagger_R}{\partial b^\dagger}\right)^{N-1}\left\langle 0\left|\frac{\partial}{\partial b^\dagger}\frac{\partial}{\partial b_R}\hat{n}_l\right|0\right\rangle,$$
$$=N!N[Z(\beta)]^{N-1}x_l^2d^l_{00}, \tag{3.3}$$

where $Z(\beta)$ is defined in Eq. (2.25) and x_l denotes the normalized mean fields in the condensate (2.9), that is,

$$x_0=1/(1+r^2)^{1/2},\quad x_1=r/(1+r^2)^{1/2}. \tag{3.4}$$

(Because it offers a more compact notation, we prefer x_1 over r in intermediate steps. In final results both will be substituted by a, i.e., $a=2x_1^2$.) Substituting Eq. (3.3) in Eq. (3.2) and coupling the d functions via Eq. (C1) to a single d^J_{00}, we obtain an integral which is of the same form as in Eq. (2.26) but with $N-1$ bosons. Thus $\langle\hat{n}_l\rangle_L$ can be written in the form

$$\langle\hat{n}_l\rangle_L=\frac{Nx_l^2}{F(N,L)}\sum_J\langle L0l0|J0\rangle^2F(N-1,J). \tag{3.5}$$

Equation (3.5) provides a typical example for the conjecture made in Sec. II C; namely, all the matrix elements can be reduced to algebraic expressions containing the normalization function. Since the algebraic manipulations required in Eq. (3.5) can be easily performed using computer algebra to any desired order in $1/N$, knowledge of $F(N,L)$ is seen to be the only factor that could limit its accuracy.

Again, the angular momentum sums (see Appendix C) and the division in Eq. (3.5) can be carried out most efficiently using MATHEMATICA. In order to demonstrate the layer structure and expose its connection with the layers in the normalization, we use Eq. (2.32) in the evaluation of Eq. (3.5) (without substituting the coefficients α_{nm} except $\alpha_{nn}=1$). The final result, complete to the order $1/N^4$, reads

$$\langle \hat{n}_l \rangle_L = N x_l^2 \Bigg\{ 1 + \frac{1}{aN}(a-\bar{l}) + \frac{1}{2(aN)^2}[2a^2 - 4a\bar{l} + \bar{l}^2 - (2a+2\bar{l})\alpha_{10} + \bar{l}\alpha_{21}] + \frac{1}{3!(aN)^3}\{6a^3 - 18\bar{l}a^2 + 9\bar{l}^2 a - \bar{l}^3 + 3$$

$$\times[-4a^2 - 4\bar{l}a + \bar{l}^2 - 2(a+\bar{l})\alpha_{10}]\alpha_{10} + 3\bar{l}(3a+\alpha_{10})\alpha_{21} - \bar{l}^2\alpha_{32} + 3(2a+\bar{l})\alpha_{20} - \bar{l}\alpha_{31}\} + \frac{1}{4!(aN)^4}\{24a^4$$

$$-96\bar{l}a^3 + 72\bar{l}^2a^2 - 16\bar{l}^3 a + \bar{l}^4 - 24(a+\bar{l})\alpha_{10}^3 - 12(4a^2 + 4\bar{l}a - \bar{l}^2)\alpha_{10}^2 - 4(18a^3 + 18\bar{l}a^2 - 9\bar{l}^2 a + \bar{l}^3)\alpha_{10}$$

$$+12(6\bar{l}a^2 + 3\bar{l}a\alpha_{10} + \bar{l}\alpha_{10}^2)\alpha_{21} - 4(4\bar{l}^2 a + \bar{l}^2\alpha_{10})\alpha_{32} + \bar{l}^3\alpha_{43} + 6[10a^2 + 4\bar{l}a - \bar{l}^2 + (6a+4\bar{l})\alpha_{10} - \bar{l}\alpha_{21}]\alpha_{20}$$

$$-4(4\bar{l}a + \bar{l}\alpha_{10})\alpha_{31} + \bar{l}^2\alpha_{42} - 4(3a+\bar{l})\alpha_{30} + \bar{l}\alpha_{41}\} + \frac{\bar{L}}{(aN)^2}\Bigg[-a + \bar{l} + \frac{1}{3aN}[-6a^2 + 12a\bar{l} - 3\bar{l}^2 + 2\bar{l} - 6a\alpha_{10}$$

$$+3(a+\bar{l})\alpha_{21} - 2\bar{l}\alpha_{32}] + \frac{1}{4!(aN)^2}\{-72a^3 + 216\bar{l}a^2 + 4\bar{l}(-27\bar{l}+16)a + 12\bar{l}^3 - 20\bar{l}^2 + 16\bar{l} - 24(3a+\bar{l})\alpha_{10}^2$$

$$+4(-24a^2 + 12a\bar{l} - 3\bar{l}^2 + 4\bar{l})\alpha_{10} + 6[10a^2 + 10\bar{l}a - \bar{l}^2 + (6a+8\bar{l})\alpha_{10} - \bar{l}\alpha_{21}]\alpha_{21} - 4\bar{l}(16a + \bar{l} + 4\alpha_{10})\alpha_{32}$$

$$+\bar{l}(9\bar{l}-4)\alpha_{43} + 36a\alpha_{20} - 4(3a+2\bar{l})\alpha_{31} + 4\bar{l}\alpha_{42}\}\Bigg] + \frac{\bar{L}^2}{4!(aN)^4}[12a^2 - 24a\bar{l} + 6\bar{l}^2 - 4\bar{l} + 12(-3a+\bar{l})\alpha_{10}$$

$$+6(6a+\bar{l})\alpha_{21} - 4(3a+5\bar{l})\alpha_{32} + 9\bar{l}\alpha_{43}]\Bigg\}. \tag{3.6}$$

Although Eq. (3.6) is derived for the one-body terms in the Hamiltonian, the same structure (i.e., the N and $\bar{L}$ dependence, and the distribution of layers in α_{nm}) persists also in the case of higher-order interactions. In order to facilitate the discussion of various terms in the expansion, we introduce a generic form for the expectation value of a ν-body scalar operator $\hat{O}$:

$$\langle \hat{O} \rangle_L = N^\nu \sum_{nm} \left(\frac{\bar{L}}{(aN)^2} \right)^n \frac{O_{nm}}{(aN)^m}, \tag{3.7}$$

where the expansion coefficients O_{nm} are functions of α_{nm} and the mean field a is as in Eq. (3.6). Note that due to cancellations between the numerator and the denominator, the $\bar{L}/N$ dependence in the normalization function has become $\bar{L}/N^2$ in Eq. (3.7). This is essential for the convergence of the series, as otherwise matrix elements for $L=N$ would become a power series in N and diverge. We refer to the $k+1$ terms in the expansion which have $n+m=k$ constant as the kth layer. The N and $\bar{L}$ dependence of the kth layer is the same as the kth power of the first layer. Thus one can consider the double expansion $1/N$ and $\bar{L}$ as a single expansion in layers. Below we discuss the significance of each layer in turn.

Zeroth layer (O_{00}): The leading term in Eq. (3.6) is the same as the mean-field result in Eq. (2.11), which establishes the validity of the mean-field theory at the limit of large N ($N\to\infty$). Naturally, O_{00} is independent of projection.

First layer (O_{01}, O_{10}): The first one gives the $1/N$ correction to the ground energy and the second gives the leading contribution to the moment of inertia. If the rotational band in question is measured only to low spins ($L<10$), knowledge of the first-layer terms is quite sufficient for its description. Note that there is no α_{nm} dependence in the first layer but that is because we used $\alpha_{nn}=1$. Otherwise, there would be α_{nn} dependence in the first layer.

Second layer (O_{02}, O_{11}, O_{20}): These terms represent, respectively, the $1/N^2$ correction to the ground energy, $1/N$ correction to the moment of inertia, and the leading-order contribution to the deviation from rigid rotor behavior. If a rotational band is known to spins $10<L<20$, this last term, which is a measure of the softness of a rotor, is essential in its description. Terms in the second layer are seen to depend on α_{nn-1}, that is, the second-layer coefficients in the normalization (see Appendix A), but no higher.

Third layer ($O_{03}, O_{12}, O_{21}, O_{30}$): The first three represent the higher-order corrections to the second-layer terms. The last one is a correction to the softness parameter which is important in description of high-spin states ($L>20$). Equation (3.6) contains only the O_{02}, O_{11} terms from the third layer, which are seen to depend on α_{nn-1} and α_{nn-2}, i.e., up to the third-layer coefficient in the normalization.

In addition, Eq. (3.6) contains the O_{04} term from the fourth layer, which depends on α_{nm} up to the fourth layer. The connection between the layers in the normalization and the matrix elements should be clear from the above discussion: In order to calculate the matrix elements up to the kth layer, one needs to know the coefficients α_{nm} up to that layer (to order $1/N^{2k}$). This is very useful in higher-order calculations as it restricts the number of terms needed in the normalization, excluding those which are most complex. Another computational advantage in using layers is that the length of terms O_{nm} increases exponentially with m, and terminating the series in m earlier reduces the amount of algebra enormously. For example, in Eq. (3.6), terms to the

second layer take only a few lines, and the bulk of the expression is occupied by the O_{03}, O_{12} terms from the third layer and O_{04} from the fourth layer. When one fits a rotational band with the form $C_0+C_1\bar{L}+C_2\bar{L}^2$, the coefficient C_0 is determined most accurately and the others are increasingly less so. In a second-layer calculation, C_0, C_1, and C_2 are evaluated to order $1/N^2$, $1/N$, and 1, respectively, which meets this hierarchical requirement in accuracy perfectly. From a practical point of view, the accuracy offered by the higher-order terms is never required. Thus, on both physical and computational grounds, use of layers is a more sensible approach than a complete calculation to a given order in $1/N$. The further utility of the layer approach will be seen later when we discuss the variational problem.

B. Ground band

Rotational bands in diatomic molecules are measured up to quite high spins ($L>20$), which necessitates calculation of the expectation value of the Hamiltonian to the third layer. As the complexity of calculations increases substantially with the order of the interaction, we will consider the one-, two-, and three-body terms in Eqs. (2.3) and (2.4) separately, in that order. The expectation value of $\hat{L}\cdot\hat{L}$ gives $\bar{L}=L(L+1)$ as expected from rotational invariance. Since it does not play any role in the dynamics of the system, it is not considered further in this section.

The expectation value for a general one-body operator has already been discussed in detail in the last subsection. Here we present the result for $\hat{n}_p$, extended to the third layer:

$$\langle\hat{n}_p\rangle_L=\frac{aN}{2}\left\{1-\frac{2-a}{aN}+\frac{\bar{L}}{(aN)^2}(2-a)\left[1+2(1-a)\left(\frac{1}{aN}+\frac{3-2a}{(aN)^2}\right)\right]-\frac{\bar{L}^2}{(aN)^4}(2-a)(1-a)\left[1+\frac{8-7a}{aN}\right]+\frac{\bar{L}^3}{(aN)^6}2(2-a)(1-a)^2\right\}. \tag{3.8}$$

For $a=1$, Eq. (3.8) reduces to

$$\langle\hat{n}_p\rangle_L=\frac{N}{2}\left(1-\frac{1}{N}+\frac{\bar{L}}{2N^2}\right), \tag{3.9}$$

in agreement with the O(4) result given in Eq. (B7). Note that after the substitution of α_{nm} in Eq. (3.6), all the complicated O_{0m} terms with $m>1$ have vanished in Eq. (3.8), leading to a finite expansion for $L=0$. This is a general feature of the ground energy that will emerge from the expectation values of all the other terms in the Hamiltonian.

There are two two-body interaction terms in Eq. (2.3). We first consider $\hat{n}_p^2$ as an example, to demonstrate the basic technique involved in the evaluation of two-body terms. To simplify the calculations, we rewrite $\hat{n}_p^2$ in the normal-ordered form

$$\hat{n}_p^2=\ :\hat{n}_p^2:+\hat{n}_p\,,\quad :\hat{n}_p^2:=\sum_{\mu\mu'}p_\mu^\dagger p_{\mu'}^\dagger p_\mu p_{\mu'}, \tag{3.10}$$

where colons denote a normal-ordered operator. Here the second term is an effective one-body operator that results from the contraction of boson operators. Since its expectation value has already been evaluated in Eq. (3.8), we need to do the calculation only for the first term. The projected expectation value for $\hat{n}_p^2$ is given by

$$\langle\hat{n}_p^2\rangle_L=\frac{1}{2N!F(N,L)}\int d\beta(\sin\beta)d_{00}^L(\beta)\times\langle 0|b^N(:\hat{n}_p^2:+\hat{n}_p)(b_R^\dagger)^N|0\rangle. \tag{3.11}$$

Using boson calculus, the matrix element for the first term in Eq. (3.11) can be evaluated as

$$\langle 0|b^N:\hat{n}_p^2:(b_R^\dagger)^N|0\rangle=N!N(N-1)[Z(\beta)]^{N-2}(x_1^2d_{00}^1)^2. \tag{3.12}$$

After substituting Eq. (3.12) in Eq. (3.11) and coupling all the d functions to a single d_{00}^J, we again recover the standard form for the β integral in Eq. (2.26) but with $N-2$ bosons. Thus $\langle\hat{n}_p^2\rangle_L$ becomes

$$\langle\hat{n}_p^2\rangle_L=\frac{a^2N(N-1)}{4F(N,L)}\sum_{lJ}\langle 1010|l0\rangle^2\langle L0l0|J0\rangle^2F(N-2,J)+\langle\hat{n}_p\rangle_L\,. \tag{3.13}$$

The rest of the algebraic manipulations in Eq. (3.13) can be carried out using MATHEMATICA, leading to the third-layer result

$$\langle\hat{n}_p^2\rangle_L=\frac{(aN)^2}{4}\left\{1-\frac{2-a}{aN}+\frac{2(2-a)}{(aN)^2}+\frac{\bar{L}}{(aN)^2}2(2-a)\times\left[1-\frac{1+a}{aN}-\frac{2+a-2a^2}{(aN)^2}\right]+\frac{\bar{L}^2}{(aN)^4}(2-a)\times\left[a+\frac{2+6a-7a^2}{aN}\right]-\frac{\bar{L}^3}{(aN)^6}2a(2-a)(1-a)\right\}. \tag{3.14}$$

The second two-body term in Eq. (2.3) is the dipole interaction, which has the normal-ordered form

$$\hat{D}\cdot\hat{D}=\ :\hat{D}\cdot\hat{D}:+3\hat{n}_s+\hat{n}_p\,. \tag{3.15}$$

The expectation value of $\hat{n}_s$ can be obtained from that of $\hat{n}_p$ using the conservation of boson number which stipulates

$$\langle\hat{n}_s\rangle_L+\langle\hat{n}_p\rangle_L=N. \tag{3.16}$$

Following the steps outlined above, the expectation value of $\hat{D}\cdot\hat{D}$ can be reduced to the form

$$\langle\hat{D}\cdot\hat{D}\rangle_L=\frac{a(2-a)N(N-1)}{2F(N,L)}\sum_{l=0}^{1}\sum_J\langle L0l0|J0\rangle^2F(N-2,J)+3\langle\hat{n}_s\rangle_L+\langle\hat{n}_p\rangle_L\,. \tag{3.17}$$

MATHEMATICA evaluation of Eq. (3.17) to the third layer gives

$$\langle \hat{D}\cdot\hat{D}\rangle_L = aN^2\Bigg\{2-a+\frac{1+2a-a^2}{aN}-\frac{\overline{L}}{(aN)^2}(2-a)\times\Bigg[2a-1-2(1-a)^2\Big(\frac{1}{aN}+\frac{3-2a}{(aN)^2}\Big)\Bigg]-\frac{\overline{L^2}}{(aN)^4}(2-a)(1-a)^2\Big[1+\frac{8-7a}{aN}\Big]+\frac{\overline{L^3}}{(aN)^6}2(2-a)(1-a)^3\Bigg\}. \tag{3.18}$$

For $a=1$, Eq. (3.18) reduces to

$$\langle \hat{D}\cdot\hat{D}\rangle_L = N^2+2N-\overline{L}, \tag{3.19}$$

in agreement with Eq. (B2), obtained from the O(4) Casimir operator.

We next consider the three-body interactions in Eq. (2.4). Of the three terms in Eq. (2.4), $\hat{n}_p\hat{L}^2$ is the easiest to evaluate because the states have good angular momentum. Its expectation value is trivially given by

$$\langle \hat{n}_p\hat{L}^2\rangle_L = \langle \hat{n}_p\rangle_L\overline{L}. \tag{3.20}$$

Calculation of the expectation value of $\hat{n}_p^3$ follows similar lines to the previous, lower-order ones. To establish the pattern, we show a few key steps here. The normal-ordered form for $\hat{n}_p^3$ is given by

$$\hat{n}_p^3 = :\hat{n}_p^3: + 3\hat{n}_p^2 - 2\hat{n}_p. \tag{3.21}$$

The intrinsic matrix element for the normal-ordered part is

$$\langle 0|b^N:\hat{n}_p^3:(b_R^\dagger)^N|0\rangle = N!N(N-1)(N-2)\times[Z(\beta)]^{N-3}(x_1^2 d_{00}^1)^3. \tag{3.22}$$

After combining the d functions and substituting the β integral, the expectation value can be reduced to the form

$$\langle \hat{n}_p^3\rangle_L = \frac{a^3N(N-1)(N-2)}{8F(N,L)}\times\sum_{ll'J}\langle 1010|l0\rangle^2\langle 10l0|l'0\rangle^2\langle L0l'0|J0\rangle^2\times F(N-3,J)+3\langle \hat{n}_p^2\rangle_L-2\langle \hat{n}_p\rangle_L. \tag{3.23}$$

Finally, MATHEMATICA evaluation of Eq. (3.23) gives the following third-layer result:

$$\langle \hat{n}_p^3\rangle_L = \frac{(aN)^3}{8}\Bigg\{1+\frac{(2-a)(2+a)}{(aN)^2}+\frac{\overline{L}}{(aN)^2}3(2-a)\times\Big[1-\frac{2+a}{aN}+\frac{10/3-2a+2a^2}{(aN)^2}\Big]+\frac{\overline{L^2}}{(aN)^4}3(2-a)\times\Big[1-\frac{2a}{N}\Big]+\frac{\overline{L^3}}{(aN)^6}(2-a)(-2+2a+a^2)\Bigg\}. \tag{3.24}$$

Comparing Eqs. (3.5), (3.13), and (3.23), it should be fairly clear how to generalize these results to even higher-order interactions in $\hat{n}_p$. The last expectation value to be considered is the second term in Eq. (2.4). We simply quote the final result here:

$$\langle \hat{n}_p\hat{D}^2+\hat{D}^2\hat{n}_p\rangle_L = a^2N^3\Bigg\{2-a+\frac{1}{aN}-\frac{(2-a)(1+a^2)}{(aN)^2}+\frac{\overline{L}}{(aN)^2}3(2-a)\Big[1-a+\frac{1-a+a^2}{aN}+\frac{2(1-a)(4/3-2a+a^2)}{(aN)^2}\Big]-\frac{\overline{L^2}}{(aN)^4}\times(2-a)\Big[1+\frac{3(1-a)(3-4a+2a^2)}{aN}\Big]+\frac{\overline{L^3}}{(aN)^6}(2-a)(1-a)(2-2a+a^2)\Bigg\}. \tag{3.25}$$

We have already commented on the general form of the $1/N$ expressions in the last subsection. Here we compare the projected energies for the one- and two-body terms with those obtained in the mean-field theory, Eq. (2.11), and make a few observations on common features of the expectation values. Rewriting the energy surface (2.11) in terms of a yields

$$E(a) = \varepsilon\frac{aN}{2}+\sigma\frac{(aN)^2}{4}\Big(1+\frac{2-a}{aN}\Big)-\kappa aN^2\Big(2-a+\frac{3-3a+a^2}{aN}\Big)+\kappa' aN. \tag{3.26}$$

Comparing Eqs. (3.8), (3.14), and (3.18) with the corresponding terms in Eq. (3.26), it is seen that the leading terms agree but the next-order $(1/N)$ terms differ. The $\hat{L}\cdot\hat{L}$ interaction forms an exceptional case in that its leading term vanishes and the remaining part in Eq. (3.26) is entirely spurious. The above example explicitly shows that the mean-field theory is valid in the large-N limit. Thus, one should consider only the leading-order terms in the energy surface and ignore the $1/N$ corrections that are not complete. An easy way to achieve this is to use the Hamiltonian in normal-ordered form in mean-field calculations. In this manner, one automatically excludes the $1/N$ terms arising from the con-

traction of boson operators, and thereby avoids potential pitfalls that could arise from odd-multipole interactions such as $\hat{L}\cdot\hat{L}$.

As remarked earlier, the ground energy ($L=0$) has a finite expansion in $1/N$, regardless of the type of interaction used. A finite expansion is usually the hallmark of an exactly solvable model as in the case of dynamical symmetries. Another remark concerns the common factors of $(2-a)$ in the moment of inertia (MOI) terms. In the limit of $a\to 2$, $r\to\infty$, which corresponds to a dissociated molecule with an infinite MOI. Hence the factors of $(2-a)$ simply ensure that no rotational excitation of such a molecule is possible. These factors arise directly from projection, and thus provide a nontrivial check on the accuracy of calculations.

C. Variation after projection

Since there is only one variational parameter in the boson system, which is to be determined from the ground band, we consider the variational problem before moving on to the vibrational bands. The simplicity of the vibron model allows an analytical solution for variation after projection, without resorting to iterative numerical techniques as is usually the case in Hartree-Bose problems (e.g., the IBM). This, in turn, permits writing of the energy expressions directly in terms of the Hamiltonian parameters, an endowment which is normally reserved for dynamical symmetries. In order to take full advantage of the $1/N$ expansion in the solution process, we first scale the strength of the interactions, so that their expectation values have the same N dependence to leading order. Further, since the dipole interaction dominates the Hamiltonian, its strength sets the energy scale of the spectrum. Thus, we factor out κN^2 from the energy expressions, and introduce the dimensionless strength parameters for the other interactions as

$$\eta_1=\frac{\varepsilon}{4N\kappa},\quad \eta_2=\frac{\sigma}{4\kappa},\quad \eta_3=\frac{3N\tau_1}{16\kappa},$$

$$\eta_3'=\frac{N\tau_2}{2\kappa},\quad \eta_3''=\frac{N\tau_3}{2\kappa}. \tag{3.27}$$

The numerical factors in Eqs. (3.27) are chosen for convenience to simplify the expressions. For small perturbations of the O(4) limit, the strength parameters η_i should all be much less than 1.

Adding all the contributions from Eqs. (3.8), (3.14), (3.18), (3.24), and (3.25), one obtains a rather lengthy expression for the ground-band energies. In discussing the variational problem, it will be more convenient to express it in a compact form. Thus, following the general form in Eq. (3.7), we rewrite the ground-band energy as

$$E_{g,L}(a)=\kappa N^2\sum_{nm}\frac{C_{nm}}{N^m}\left(\frac{\overline{L}}{N^2}\right)^n. \tag{3.28}$$

The coefficients C_{nm} in Eq. (3.28) can be read off from the respective contributions in the last subsection. For example, the coefficients for the zeroth and first layers are given by

$$\begin{aligned}
C_{00}&=-a(2-a)+2\eta_1 a+\eta_2 a^2+2\eta_3 a^3/3+2\eta_3' a^2(2-a),\\
C_{01}&=-(1+2a-a^2)-2\eta_1(2-a)-\eta_2 a(2-a)+2\eta_3' a,\\
C_{10}&=(2-a)[(2a-1)/a+2\eta_1/a+2\eta_2+2\eta_3 a+6\eta_3']\\
&\quad+\eta_3'' a,
\end{aligned} \tag{3.29}$$

where we have substituted the scaled parameters from Eqs. (3.27). The minimum of the ground energy is obtained from

$$\frac{dE_{g,L}(a)}{da}=0, \tag{3.30}$$

which can be solved algebraically using an ansatz similar to Eq. (3.28):

$$a=\sum_{nm}\frac{a_{nm}}{N^m}\left(\frac{\overline{L}}{N^2}\right)^n. \tag{3.31}$$

Use of the layer approach again simplifies solution of the variational equation. Substituting the ansatz (3.31) in Eq. (3.30), it can be shown that each layer leads to an independent set of equations. Thus starting from the zeroth layer, one can construct the solution layer by layer. For the leading order (zeroth layer), one has the Hartree-Bose equation

$$\left.\frac{dC_{00}}{da}\right|_{a_{00}}=0. \tag{3.32}$$

In the following, we will denote a_{00} as a_0 for notational convenience. Using the expression for C_{00}, Eqs. (3.29), in Eq. (3.32), we obtain the following quadratic equation for a_0:

$$-1+\eta_1+(1+\eta_2+4\eta_3')a_0+(\eta_3-3\eta_3')a_0^2=0. \tag{3.33}$$

Since $a\geqslant 0$, we take the positive root of this equation:

$$\begin{aligned}
a_0=\frac{1}{2(\eta_3-3\eta_3')}\{&-(1+\eta_2+4\eta_3')\\
&+[(1+\eta_2+4\eta_3')^2+4(1-\eta_1)(\eta_3-3\eta_3')]^{1/2}\}.
\end{aligned} \tag{3.34}$$

This solution leads to an indeterminate result when the cubic terms vanish. To obtain a more transparent result, we expand it for small cubic strength:

$$\begin{aligned}
a_0=\frac{1-\eta_1}{1+\eta_2+4\eta_3'}\Bigg[&1-\frac{(1-\eta_1)(\eta_3-3\eta_3')}{(1+\eta_2+4\eta_3')^2}\\
&+2\left(\frac{(1-\eta_1)(\eta_3-3\eta_3')}{(1+\eta_2+4\eta_3')^2}\right)^2-\cdots\Bigg].
\end{aligned} \tag{3.35}$$

For the one- and two-body parts of the Hamiltonian, i.e., for $\eta_3=\eta_3'=0$ in Eq. (3.35), one obtains a very simple result for a_0:

$$a_0=(1-\eta_1)/(1+\eta_2). \tag{3.36}$$

When all $\eta\ll 1$, corresponding to small perturbations of the O(4) limit, Eq. (3.35) gives to leading order

$$a_0 = 1 - \eta_1 - \eta_2 - \eta_3 - \eta_3', \tag{3.37}$$

which explains the choice of the numerical factors in Eq. (3.27). With the exception of η_3'', all the symmetry-breaking terms with equal scaled strength η lead to an equivalent change in the size parameter.

Once a_0 is determined, the next layers in the solution, a_{01} and a_{10}, are obtained by solving the respective set of equations for the first layer:

$$\left.\frac{dC_{00}}{da}\right|_{a_0 + a_{01}/N} = -\frac{1}{N}\left.\frac{dC_{01}}{da}\right|_{a_0},$$

$$\left.\frac{dC_{00}}{da}\right|_{a_0 + a_{10}\bar{L}/N^2} = -\frac{\bar{L}}{N^2}\left.\frac{dC_{10}}{da}\right|_{a_0}. \tag{3.38}$$

Upon substituting the mean fields in the derivatives in Eqs. (3.38), the leading order vanishes by virtue of the Hartree-Bose equation (3.32). The next order leads to trivial linear equations for a_{01} and a_{10} that can be solved to give

$$a_{01} = \frac{1 - \eta_1 + \eta_2 - \eta_3' - (1+\eta_2)a_0}{1 + \eta_2 + 4\eta_3' + 2(\eta_3 - 3\eta_3')a_0},$$

$$a_{10} = \frac{1 - (1-2\eta_1)/a_0^2 + \eta_2 - 2\eta_3(1-a_0) + 3\eta_3' - \eta_3''}{1 + \eta_2 + 4\eta_3' + 2(\eta_3 - 3\eta_3')a_0}. \tag{3.39}$$

Substituting a_0 from Eq. (3.34), the coefficients a_{01} and a_{10} can be determined directly in terms of the Hamiltonian parameters. These general expressions are somewhat complicated, and so we will not quote them here. When only the one- and two-body parts are considered, they reduce to particularly simple forms given by

$$a_{01} = \frac{\eta_2}{1+\eta_2}, \quad a_{10} = \frac{\eta_1^2 + 2\eta_1\eta_2 - \eta_2}{(1-\eta_1)^2}. \tag{3.40}$$

A question of general interest here is the the difference between variation after and before projection (VAP and VBP) results. In VBP, one substitutes the leading-order mean field (a_0), obtained from the Hartree-Bose equation, in the energy expression (3.28). Whereas in VAP, the full solution for the mean field (3.31) is used. Thus, the difference between VAP and VBP arises from the contribution of the higher-order mean fields to the ground energy. From the Taylor expansion of $E_{g,L}(a)$ and the Hartree-Bose condition (3.32), it is clear that the contribution of the first-layer mean fields to the first layer in the ground energy vanishes, and these correction terms due to VAP appear only at the second and higher layers. This holds in general for all layers, in that the corrections due to a given layer in the mean fields appear in the next and higher levels in the energy. Therefore, VAP and VBP give the same results for the first layer (i.e., leading terms in band excitation energies and moment of inertia), but differ in the second and higher layers.

The above argument indicates that for the third-layer expansion considered here, one needs at most the second-layer mean fields a_{02}, a_{11}, and a_{20}. These are obtained from the set of equations

$$\left.\frac{dC_{00}}{da}\right|_{a_0 + a_{01}/N + a_{02}/N^2} = -\frac{1}{N}\left.\frac{dC_{01}}{da}\right|_{a_0 + a_{01}/N} - \frac{1}{N}\left.\frac{dC_{02}}{da}\right|_{a_0},$$

$$\left.\frac{dC_{00}}{da}\right|_{a_0 + a_{10}\bar{L}/N^2 + a_{20}\bar{L^2}/N^4} = -\frac{\bar{L}}{N^2}\left.\frac{dC_{10}}{da}\right|_{a_0 + a_{10}\bar{L}/N^2} - \frac{\bar{L^2}}{N^4}\left.\frac{dC_{20}}{da}\right|_{a_0},$$

$$\left.\frac{dC_{00}}{da}\right|_{a_0 + a_{01}/N + a_{10}\bar{L}/N^2 + a_{11}\bar{L}/N^3} = -\frac{1}{N}\left.\frac{dC_{01}}{da}\right|_{a_0 + a_{10}\bar{L}/N^2} - \frac{\bar{L}}{N^2}\left.\frac{dC_{10}}{da}\right|_{a_0 + a_{01}/N} - \frac{\bar{L}}{N^3}\left.\frac{dC_{11}}{da}\right|_{a_0}. \tag{3.41}$$

Again, after substituting the mean fields, the zeroth- and first-layer parts of these equations vanish by virtue of Eqs. (3.32) and (3.38), leaving behind trivial linear equations for the second-layer mean fields.

The resulting mean fields and the energy expressions are rather lengthy when the cubic terms are included. Therefore, in presenting the complete third-layer results, we prefer to restrict ourselves to the one- and two-body terms in the Hamiltonian. This will make the comparisons between VAP and VBP easier. To this end, we first give the explicit expression for $E_{g,L}(a)$:

$$E_{g,L}(a) = \kappa N^2 \Bigg\{ a(a-2+2\eta_1+a\eta_2) + \frac{1}{N}[(-1-2a+a^2) - 2(2-a)\eta_1 - a(2-a)\eta_2] + \frac{2}{N^2}(2-a)\eta_2 + \frac{\bar{L}}{N^2}\frac{2-a}{a}\Big[2a - 1 + 2\eta_1 + 2a\eta_2 - \frac{2}{aN}[(1-a)(1-a-2\eta_1) + a(1+a)\eta_2] - \frac{2}{(aN)^2}[(1-a)(3-2a)(1-a-2\eta_1) + a(2+a-2a^2)\eta_2]\Big] + \frac{\bar{L^2}}{N^4}\frac{2-a}{a^3}\Big[(1-a)(1-a-2\eta_1) + a^2\eta_2 + \frac{1}{aN}[(1-a)(7-8a)(1-a-2\eta_1) + a(2+6a-7a^2)\eta_2]\Big] - \frac{\bar{L^3}}{N^6}\frac{2}{a^5}(2-a)(1-a)[(1-a)(1-a-2\eta_1) + a^2\eta_2]\Bigg\}. \tag{3.42}$$

The solution of the variational problem for Eq. (3.42) has already been given in Eqs. (3.36) and (3.40) for the zeroth and first layers, respectively. Extending this solution for a to the second layer gives

$$a=\frac{1-\eta_1}{1+\eta_2}+\frac{1}{N}\frac{\eta_2}{1+\eta_2}+\frac{\overline{L}}{N^2}\frac{1}{(1-\eta_1)^2}\left[\eta_1^2+2\eta_1\eta_2-\eta_2+\frac{1}{N}\frac{2}{1-\eta_1}[\eta_1^2(1+\eta_1+4\eta_2)-\eta_2+\eta_2^2(3\eta_1-2)]\right]$$
$$+\frac{\overline{L^2}}{N^4}\frac{1+\eta_2}{(1-\eta_1)^5}(\eta_1^2+2\eta_1\eta_2-\eta_2)(\eta_1^2-\eta_1\eta_2-3\eta_1-\eta_2). \tag{3.43}$$

When $\eta_1=\eta_2=0$, Eq. (3.43) reduces to $a=1$, consistent with the O(4) limit. Thus, there is no difference between VAP and VBP in the O(4) limit. Finally, substituting Eq. (3.43) in Eq. (3.42), we obtain the following expression for the ground-band energies, directly in terms of the Hamiltonian parameters:

$$E_{g,L}=\kappa N^2\left\{-\frac{1}{1+\eta_2}\left[(1-\eta_1)^2+\frac{1}{N}(2+2\eta_1+\eta_1^2+2\eta_1\eta_2+3\eta_2)-\frac{1}{N^2}(2+2\eta_1+3\eta_2)\eta_2+\frac{1}{N^3}\eta_2^2\right]+\frac{\overline{L}}{N^2}\frac{1}{1-\eta_1}\left[1+\eta_1\right.\right.$$
$$+2\eta_2+\frac{1}{N}\frac{2}{1-\eta_1}[(1+\eta_1)\eta_1^2-(2-\eta_1-4\eta_1^2)\eta_2-(3-4\eta_1)\eta_2^2]+\frac{1}{N^2}\frac{2}{(1-\eta_1)^2}[(1+\eta_1)(1+2\eta_1)\eta_1^2-(1+3\eta_1$$
$$\left.-6\eta_1^2-12\eta_1^3)\eta_2-(3+6\eta_1-20\eta_1^2)\eta_2^2-(5-8\eta_1)\eta_2^3]\right]-\frac{\overline{L^2}}{N^4}\frac{1}{(1-\eta_1)^4}\left[(1+\eta_2)^2(\eta_1^2+2\eta_1\eta_2-\eta_2)+\frac{1}{N}\frac{1+\eta_2}{1-\eta_1}\right.$$
$$\left.\times[(1+7\eta_1+4\eta_1^2-4\eta_1^3)\eta_1^2-(1+7\eta_1-13\eta_1^2-31\eta_1^3+16\eta_1^4)\eta_2-(3+17\eta_1-52\eta_1^2+16\eta_1^3)\eta_2^2-(6-10\eta_1)\eta_2^3]\right]$$
$$\left.+\frac{\overline{L^3}}{N^6}\frac{2\eta_1(1+\eta_2)^4}{(1-\eta_1)^7}(\eta_1^2+2\eta_1\eta_2-\eta_2)\right\}. \tag{3.44}$$

Equation (3.44) is an exact result to the given order. We have carried out a numerical analysis of the diagonalization results for the Hamiltonian (2.3), and directly verified that the N and $\overline{L}$ dependence of the ground-band energies are as given in Eq. (3.44). This agreement with the diagonalization results also confirms that Eq. (3.44) is free from computational errors.

The energy difference between VAP and VBP results is obtained by subtracting Eq. (3.42) with $a=a_0$ from Eq. (3.44). To the second layer, which is of most interest, it is given by

$$E_{g,L}-E_{g,L}(a_0)=-\kappa N^2\left(\frac{1}{N^2}\frac{\eta_2^2}{1+\eta_2}+\frac{\overline{L}}{N^3}\frac{2\eta_2(\eta_1^2+2\eta_1\eta_2-\eta_2)}{(1-\eta_1)^2}\right.$$
$$\left.+\frac{\overline{L^2}}{N^4}\frac{(1+\eta_2)(\eta_1^2+2\eta_1\eta_2-\eta_2)^2}{(1-\eta_1)^4}\right). \tag{3.45}$$

Thus, as expected, VAP leads to a lower ground energy than VBP. Note also that for $\eta_2=0$, the difference in the ground energy and MOI ($\overline{L}$) terms vanish. In fact, the equivalence of VAP and VBP for these terms holds also in the higher layers. Thus breaking of the O(4) limit with the $\hat{n}_p$ term constitutes a special case, as it partially preserves the complete equivalence of VAP and VBP found in the O(4) limit.

As a final remark on the ground-band energies (3.44), we discuss the MOI systematics and its correlation with the size parameter a or r. [Note that for small perturbations of the O(4) limit $a\approx r$.] From Eqs. (3.35)–(3.37), it is seen that the equilibrium size gets smaller for positive values of η and larger for negative values. Inspection of the MOI term in Eq. (3.44) shows that it also gets smaller for positive η and larger for negative η. Thus the two quantities are correlated as in the geometrical models; a larger size leads to a larger MOI. The same correlation holds also for the cubic terms $\hat{n}_p^3$ and $\hat{n}_p\hat{D}^2+\hat{D}^2\hat{n}_p$ but not for the $\hat{L}^2$ and $\hat{n}_p\hat{L}^2$ terms. In fact, the $\hat{L}^2$ term is completely divorced from the dynamics of the system (the MOI remains constant as a or r changes), and the $\hat{n}_p\hat{L}^2$ term has the wrong dynamic dependence on r (the MOI decreases as r increases). Thus caution should be exercised in phenomenological uses of these terms. It would be better if they could be avoided altogether, but certainly they should not play a dominant role in description of the MOI.

D. Vibrational bands

Calculations for the vibrational bands follow much the same lines as in the ground band;, namely, (i) matrix element of a given interaction is evaluated in the intrinsic frame using boson calculus, (ii) all the resulting d functions are combined to a single d^J_{00}, and (iii) the normalization function (2.32) with the appropriate N is substituted for the resulting β integrals. The rest of the calculations require standard algebraic manipulations that can be carried out most efficiently

using MATHEMATICA. The only difference is that there are many more terms to be evaluated and the amount of angular momentum algebra in each term gets longer. As a rule of thumb, the complexity of calculations grows exponentially with the vibrational number v. Nevertheless, the final expressions obtained are as compact as those for the ground band. For reasons of economy, we skip all the lengthy technical details of the intermediate steps, and present directly the final results.

For $v \ll N$, the changes in structure between two neighboring bands are very similar, irrespective of the value of v. Thus to get a picture of how the band structure changes with increasing v, it is quite sufficient to compare $v=0$ and $v=1$ bands. To this end, we have repeated the ground-band calculations presented in Sec. III B for the $v=1$ band. Below, we present the third-layer results without further explanations. The expectation value of the one-body operator is given by

$$\langle \hat{n}_p \rangle_{1,L} = \frac{aN}{2}\left\{ 1 - \frac{1}{N} + \frac{\overline{L}}{(aN)^2}(2-a)\left[1 + \frac{2(3-a)}{aN} + \frac{2(5-a)(3-2a)}{(aN)^2} \right] - \frac{\overline{L^2}}{(aN)^4}(2-a)(1-a)\left[1 + \frac{3(8-3a)}{aN} \right] + \frac{\overline{L^3}}{(aN)^6} 2(2-a)(1-a)^2 \right\}. \tag{3.46}$$

Substituting $a=1$ in Eq. (3.46) reproduces the O(4) result given in Eq. (B7). For the two-body operators, we obtain

$$\langle \hat{n}_p^2 \rangle_{1,L} = \frac{(aN)^2}{4}\left\{ 1 + \frac{6-5a}{aN} + \frac{2a}{(aN)^2} + \frac{\overline{L}}{(aN)^2} 2(2-a) \times \left[1 + \frac{3(1-a)}{aN} + \frac{10-21a+6a^2}{(aN)^2} \right] + \frac{\overline{L^2}}{(aN)^4}(2-a)\left[a - \frac{6-30a+13a^2}{aN} \right] - \frac{\overline{L^3}}{(aN)^6} 2a(2-a)(1-a) \right\}, \tag{3.47}$$

$$\langle \hat{D}\cdot\hat{D} \rangle_{1,L} = aN^2\left\{ 2 - a + \frac{3-10a+5a^2}{aN} - \frac{\overline{L}}{(aN)^2}(2-a) \times \left[2a - 1 - 6(1-a)^2\left(\frac{1}{aN} + \frac{5-2a}{(aN)^2} \right) \right] - \frac{\overline{L^2}}{(aN)^4}(2-a)(1-a)^2\left[1 + \frac{24-13a}{aN} \right] + \frac{\overline{L^3}}{(aN)^6} 2(2-a)(1-a)^3 \right\}. \tag{3.48}$$

Again, substituting $a=1$ in Eq. (3.48), one recovers the Casimir result given in Eq. (B2). The expectation values of the three-body operators are given by

$$\langle \hat{n}_p^3 \rangle_{1,L} = \frac{(aN)^3}{8}\left\{ 1 + \frac{6(3-2a)}{aN} + \frac{(4-18a+11a^2)}{(aN)^2} - \frac{4a}{(aN)^3} + \frac{\overline{L}}{(aN)^2} 3(2-a)\left[1 + \frac{6-7a}{aN} + \frac{2(41/3-19a+7a^2)}{(aN)^2} \right] + \frac{\overline{L^2}}{(aN)^4} 3(2-a)\left[1 - \frac{2(5-3a)}{N} \right] + \frac{\overline{L^3}}{(aN)^6}(2-a)(-2+2a+a^2) \right\}, \tag{3.49}$$

$$\langle \hat{n}_p\hat{D}^2 + \hat{D}^2\hat{n}_p \rangle_{1,L} = a^2N^3\left\{ 2 - a + \frac{3(5-10a+4a^2)}{aN} - \frac{a(-15+28a-11a^2)}{(aN)^2} + \frac{\overline{L}}{(aN)^2} 3(2-a)\left[1 - a + \frac{5-11a+7a^2}{aN} + \frac{2(1-a)(34/3-18a+7a^2)}{(aN)^2} \right] - \frac{\overline{L^2}}{(aN)^4}(2-a)\left[1 + \frac{33-71a+60a^2-18a^3}{aN} \right] + \frac{\overline{L^3}}{(aN)^6}(2-a)(1-a)(2-2a+a^2) \right\}. \tag{3.50}$$

Combining the various expectation values above, and substituting the value of a, Eq. (3.43), obtained from the VAP procedure, one obtains an analytical expression for the $v=1$ band energies $E_{1,L}$ similar to Eq. (3.44) for the ground band. We do not present this long formula here because it is of limited use and it can be easily reproduced. For purposes of comparison of different bands, the original expressions in terms of a are actually more convenient.

Finally, we present similar results for the $v=2$ band. Our aim here is to confirm the conjecture made above about the change of structure in neighboring bands. Since the calculations are very laborious to carry out to the third layer, we will be content with the second-layer results. This will be seen to be sufficient for our purposes. The expectation values of the one- and two-body operators to the second layer are given by

$$\langle \hat{n}_p \rangle_{2,L} = \frac{aN}{2}\left\{ 1 + \frac{2-3a}{N} + \frac{\overline{L}}{(aN)^2}(2-a)\left[1 + \frac{2(5-a)}{aN}\right] - \frac{\overline{L^2}}{(aN)^4}(2-a)(1-a)\right\}, \tag{3.51}$$

$$\langle \hat{n}_p^2 \rangle_{2,L} = \frac{(aN)^2}{4}\left\{ 1 + \frac{14-11a}{aN} + \frac{2(2-9a+6a^2)}{(aN)^2} + \frac{\overline{L}}{(aN)^2}2(2-a)\left[1 + \frac{7-5a}{aN}\right] + \frac{\overline{L^2}}{(aN)^4}a(2-a)\right\}, \tag{3.52}$$

$$\langle \hat{D}\cdot\hat{D} \rangle_{2,L} = aN^2\left\{ 2 - a + \frac{5-22a+11a^2}{aN} - \frac{4a(1-6a+3a^2)}{(aN)^2} - \frac{\overline{L}}{(aN)^2}(2-a)\left[2a - 1 - \frac{10(1-a)^2}{aN}\right] - \frac{\overline{L^2}}{(aN)^4}(2-a)(1-a)^2\right\}. \tag{3.53}$$

Equations (3.51) and (3.53) reproduce the O(4) results given in Eqs. (B7) and (B2), respectively.

In the remaining part of this section, we contrast the energy expressions obtained for the ground and vibrational bands, and comment on their general features. An immediate observation is that the leading term in each power of $\overline{L}$ (i.e., C_{n0}) is the same in all bands. The next-order terms C_{n1}, which provide the $1/N$ correction to the former, differ from band to band, but the difference between neighboring bands remains constant. That is, $C_{n1}(v=1)-C_{n1}(v=0)=C_{n1}(v=2)-C_{n1}(v=1)$. Only in the $1/N^2$ correction terms (C_{n2}) do the differences between neighboring bands vary. For example, for the one- and two-body Hamiltonian (2.3), the second-order energy difference describing anharmonicity is given by

$$E_{g,L} - 2E_{1,L} + E_{2,L} = 4\kappa[1 - 6a + 3a^2 + \eta_2(2 - 6a + 3a^2)]. \tag{3.54}$$

Substituting a from Eq. (3.40), we obtain

$$E_{g,L} - 2E_{1,L} + E_{2,L} = \frac{-4\kappa}{1+\eta_2}[2 - 3\eta_1^2 + \eta_2(3 - 6\eta_1 - 2\eta_2)]. \tag{3.55}$$

Implications of these observations for level energies are as follows: (i) Vibrational band energies increase linearly with v to leading order, and there are small anharmonic effects of order $1/N$, and (ii) the MOI of all bands are the same to leading order, and its variation among different bands is of order $1/N$. Both of these features are in accordance with experimental systematics, as will be discussed in more detail in Sec. V.

IV. ELECTROMAGNETIC TRANSITIONS

In this section, we use the projected states to derive analytic expressions for various electromagnetic transitions, which provide sensitive tests for the wave functions. In contrast to energy levels, transition intensities are not measured very accurately. Therefore, a first-layer calculation is usually sufficient in most cases. Reduced matrix elements of a tensor operator $T^{(k)}$ between projected intrinsic states with $K=0$ are calculated using [4]

$$\langle v', L' \| \hat{T}^{(k)} \| v, L \rangle = \frac{\hat{L}'(2L+1)}{2[\mathcal{N}(N,v',L')\mathcal{N}(N,v,L)]^{1/2}} \sum_{\mu} \langle L\mu k - \mu | L' 0 \rangle \times \int_0^{\pi} d\beta \, \sin\beta d^L_{\mu 0}(\beta) \langle v' | \hat{T}^{(k)}_{-\mu} e^{-i\beta \hat{L}_y} | v \rangle, \tag{4.1}$$

where $\hat{L} = [2L+1]^{1/2}$. Here and in the following, the N quantum number is suppressed since it is a constant.

A. Infrared transitions

We first discuss the in-band electric dipole transitions using the one-body operator $\hat{D}$. Applying the boson calculus and projection techniques to Eq. (4.1), we obtain for transitions in the ground band

$$\langle 0, L' \| \hat{D} \| 0, L \rangle = N\hat{L}\langle L\,0\,1\,0 | L'\,0\rangle [a(2-a)]^{1/2} \times \frac{F(N-1,L) + F(N-1,L')}{2[F(N,L)F(N,L')]^{1/2}}. \tag{4.2}$$

Equation (4.2) shows that, like in the case of band energies, the transition matrix elements can also be reduced to forms containing the normalization function. Thus, they can be evaluated to any order in $1/N$ using MATHEMATICA. Here, we present the first-layer results as these are sufficiently accurate for practical purposes:

$$\langle 0, L' \| \hat{D} \| 0, L \rangle = N\hat{L}\langle L\,0\,1\,0 | L'\,0\rangle [a(2-a)]^{1/2} \times \left[1 + \frac{1}{N} - \frac{(\overline{L'} - \overline{L})^2}{8(aN)^2}(2a-1)\right]. \tag{4.3}$$

In obtaining this expression, we have used the relationship $\overline{L'} + \overline{L} = (\overline{L'} - \overline{L})^2/2$ which holds for $L' = L \pm 1$. For $a=1$, Eq. (4.3) reproduces the O(4) result given in Eq. (B8) to the given order. The final result follows upon substituting the VAP solution for a in Eq. (4.3). As the general result is somewhat complicated, we give here the expression for the one-body symmetry breaking with $L' = L+1$:

$$\langle 0, L+1 \| \hat{D} \| 0, L \rangle = N(L+1)^{1/2}(1-\eta_1^2)^{1/2} \times \left[1 + \frac{1}{N} - \frac{L(L+2)}{2N^2}\frac{1 - 2\eta_1 - \eta_1^2}{(1-\eta_1)^3(1+\eta_1)}\right]. \tag{4.4}$$

For small perturbations of the O(4) limit, $a_0=1-\Sigma_i \eta_i$, and the above result can be easily generalized to include other symmetry-breaking terms. In-band transition matrix elements in vibrational bands exhibit a similar structure as in the energy expectation values; namely, the leading term in each power of spin remains the same and the $1/N$ corrections vary with bands. Thus, in going from the ground band to the vibrational band v, the only change in Eqs. (4.3) and (4.4) is that the term $1/N$ is replaced by $(1-2v)/N$. The effect of symmetry breaking on in-band transitions is seen to be marginal. The change in the leading term in Eq. (4.4) can be absorbed in the dipole charge, and the small change in the $1/N^2$ term does not have any experimental consequence.

We next discuss the interband transitions which are very sensitive to changes in the vibrational quantum number. For the $\Delta v=1$ transition from the ground band, a calculation similar to Eq. (4.3) yields

$$\langle 1,L'\|\hat{D}\|0,L\rangle=\sqrt{N}\hat{L}\langle L010|L'0\rangle(a-1)\times\left[1-\frac{1}{2aN}(\overline{L'}-\overline{L}-a)\right]. \quad (4.5)$$

This expression vanishes in the O(4) limit when $a=1$. For the one-body symmetry breaking with $L'=L+1$, Eq. (4.5) becomes

$$\langle 1,L+1\|\hat{D}\|0,L\rangle=-[N(L+1)]^{1/2}\eta_1\left[1-\frac{2L+1+\eta_1}{2N(1-\eta_1)}\right]. \quad (4.6)$$

The corresponding leading-order expression for the $\Delta v=2$ transition from the ground band is given by

$$\langle 2,L+1\|\hat{D}\|0,L\rangle=\frac{4\sqrt{2}\,\eta_1^2(1-\eta_1^2)^{1/2}}{N^2(1-\eta_1)^3}(L+1)^{3/2}. \quad (4.7)$$

Comparing the above matrix elements with those obtained in the mean-field theory, Eq. (2.16), it is seen that the leading-order results agree as in the case of energies. Projection yields a nonzero result for the $\Delta v=2$ transition but this is only in the $1/N^2$ term of the series, which is too small to have any practical value. Experimentally, the $v\rightarrow 0$ transitions are 10^v smaller than the ground ones which requires roughly a drop of $N^{v/2}$ in the matrix elements. That is, a leading term of order 1 is needed in Eq. (4.7) to explain the data.

The preceding examples demonstrate that the one-body dipole operator is not sufficient to describe the vibrational transitions even with symmetry breaking. To show the effect of the higher-order terms, we calculate the same matrix elements with the two-body operator in Eq. (2.5):

$$\langle 0,L+1\|\hat{n}_p\hat{D}+\hat{D}\hat{n}_p\|0,L\rangle=N^2(L+1)^{1/2}[a(2-a)]^{1/2}\times\left[a-\frac{1-a}{N}+\frac{L(L+2)}{2aN^2}(5-4a)\right], \quad (4.8)$$

$$\langle 1,L+1\|\hat{n}_p\hat{D}+\hat{D}\hat{n}_p\|0,L\rangle=N^{3/2}(L+1)^{1/2}\left[a(2a-3)+\frac{1}{2N}\times[2L(1-a)+(4-7a+2a^2)]\right], \quad (4.9)$$

$$\langle 2,L+1\|\hat{n}_p\hat{D}+\hat{D}\hat{n}_p\|0,L\rangle=\sqrt{2}N(L+1)^{1/2}(1-a)\left[1-\frac{L}{aN}\right]. \quad (4.10)$$

The relative N dependence in the above expressions is now consistent with the data so that one can attempt to use them to describe the dipole transitions among the $v=0$, 1, and 2 bands. It should be emphasized that the intrinsic matrix element of the two-body operator vanishes for the $3\rightarrow 0$ transition, and one needs a three-body operator for its description. In general, a v-body operator is required to describe the $v\rightarrow 0$ transition. As suggested in Ref. [8], use of the exponential form (2.6), which includes all the powers of $\hat{n}_p$ in the dipole operator, is the most practical way in dealing with transitions involving higher-vibrational bands.

Here, it is of interest to comment on the spin-dependent terms in vibrational transitions which arise from rotation-vibration interactions. These terms are represented by Mikhailov plots in collective nuclei and Herman-Wallis forms in molecules. The spin-dependent terms in $\Delta v\neq 0$ transitions are seen to vanish in the O(4) limit in all cases, even when the matrix element itself is nonzero. To generate them in the O(4) limit, one needs to include the term $i[\hat{L}\hat{D}'-\hat{D}'\hat{L}]^{(1)}$ in the dipole operator, where $\hat{D}'$ corresponds to the conjugate momentum operator. In the IBM, breaking of the SU(3) symmetry was shown to provide a natural explanation for spin-dependent terms in interband transitions of collective nuclei [22]. Further, these terms exhibit a characteristic $1/N$ dependence as in Eqs. (4.9) and (4.10) (which, incidentally, provide the best signatures for finite N effects in the IBM). The $1/N$ dependence of the slope in Herman-Wallis form gives the right order of magnitude when compared to the data. Hence breaking of the O(4) symmetry may explain the spin dependence in vibrational transitions without the need for an extra term in the dipole operator.

B. Raman transitions

The available data on Raman transitions are rather scarce, and so we limit their discussion to a few examples. The ground-band matrix element of the quadrupole operator (2.8) can be reduced to the form

$$\langle 0,L'\|\hat{Q}\|0,L\rangle=\frac{\sqrt{5}aN\hat{L}\hat{L}'}{2[F(N,L')F(N,L)]^{1/2}}\sum_J\langle 10L'0|J0\rangle\times\langle L010|J0\rangle\begin{Bmatrix}1 & L' & J\\ L & 1 & 2\end{Bmatrix}F(N-1,J), \quad (4.11)$$

TABLE I. Experimental values for the ratios considered in Sec. V. The data are from Ref. [23] and listed in order of increasing MOI. The O(4) values (with $\kappa'=0$) are shown at the top row for reference. C_1 is in cm^{-1}.

Molecule	N	C_1	$\Delta E/NC_1$	N^2C_2/C_1	N^4C_3/C_1	$N\Delta C_1/C_1$	$N\Delta C_2/C_2$
O(4)		κ	4.00	0	0	0	
^{1}H ^{19}F	44	20.6	4.38	−0.200	0.029	−1.65	−1.2
^{1}H ^{35}Cl	55	10.1	5.17	−0.158		−1.60	−0.70
^{1}H ^{81}Br	57	8.35	5.38	−0.134	0.010	−1.58	−0.51
^{12}C ^{16}O	161	1.92	6.92	−0.0825	0.002	−1.51	
^{9}Be ^{16}O	124	1.64	7.19	−0.0768	0.002	−1.44	−0.15
^{32}S ^{16}O	202	0.718	7.85	−0.0642		−1.69	
^{27}Al ^{16}O	138	0.638	11.0	−0.0325		−1.30	2.5
^{27}Al ^{19}F	166	0.550	8.68	−0.0526		−1.51	−0.24
^{27}Al ^{32}S	183	0.279	12.0	−0.0264		−1.31	
^{27}Al ^{35}Cl	245	0.243	8.02	−0.0618	−0.001	−2.02	−0.52
^{27}Al ^{79}Br	293	0.158	8.11	−0.0613	−0.001	−1.85	−0.52

where the curly brackets denote the 6-j symbol. The angular momentum algebra in evaluation of Eq. (4.11) is more complicated due to the presence of the 6-j symbol. For the first layer, these are available [4], and one obtains from Eq. (4.11)

$$\langle 0,L'\|\hat{Q}\|0,L\rangle=\frac{aN}{2}\hat{L}\langle L020|L'0\rangle\left[1+\frac{a+1}{aN}-\frac{(\overline{L'}-\overline{L})^2}{16aN^2}\right]. \tag{4.12}$$

Substituting $L'=L+2$, L and $L-2$ in Eq. (4.12), expressions for the so-called S, O, and Q branches in Raman intensities can be obtained. As a final example, we give the first-layer result for the $1\rightarrow 0$ Raman transition:

$$\langle 1,L'\|\hat{Q}\|0,L\rangle=\frac{-1}{2}\sqrt{N}\hat{L}\langle L020|L'0\rangle \times\left[1-\frac{1}{2aN}(\overline{L'}-\overline{L}-a)\right]. \tag{4.13}$$

Equations (4.12) and (4.13) have a similar structure to the corresponding matrix elements for infrared transitions, Eqs. (4.3) and (4.5). Neither expression vanishes in the O(4) limit, and therefore, symmetry breaking does not play an important role in these Raman transitions.

V. APPLICATIONS TO MOLECULAR SPECTRA

The analytical $1/N$ expansion formulas derived in the previous sections greatly facilitate systematic study of diatomic molecules in the framework of the vibron model. As mentioned in the Introduction, past applications of the vibron model to molecular spectra have mostly followed the path of the symmetry-preserving approach. A primary aim of this study is to assess whether the alternative, symmetry-breaking approach can provide a more economical and realistic representation of spectroscopic data. In order to establish a reference point and motivate this study, we first compare a few key observables in some typical diatomic molecules with the O(4) predictions (see Table I). The quantities in Table I follow from the definitions of the ground and first vibrational band energies as

$$E_{g,L}=C_1\overline{L}+C_2\overline{L^2}+C_3\overline{L^3},$$
$$E_{1,L}=\Delta E+C_1'\overline{L}+C_2'\overline{L^2}+C_3'\overline{L^3}. \tag{5.1}$$

The other differential quantities are defined as $\Delta C_i=C_i'-C_i$. The data are extracted from the Dunham parameters given in Ref. [23]. The boson numbers are determined from the anharmonicity parameters using the relationship $N+2=\omega_e/\omega_e x_e$ [3]. In a few cases where these parameters are not well determined (e.g., AlO and AlS), N appears to be underestimated. While use of a larger N in these cases would have avoided the large fluctuations, leading to a smoother trend in the ratios, we have decided against it as it would be a rather *ad hoc* procedure.

The reasons for the particular way the data are presented are as follows. As stressed before, κ is a scale parameter and it is best determined from the first vibrational energy ΔE. By using ratios of the quantities in Eq. (5.1), we eliminate this trivial scale parameter from the discussions. Second, the factors of N are chosen such that the ratios are independent of N. (Here we limit ourselves to the leading-order terms in $1/N$ which is sufficient for a qualitative discussion.) Thus the ratios provide universal parameters for a description of the spectra of diatomic molecules, independent of the scale parameters. The usefulness of the ratios becomes apparent when one contrasts their range of variation with those of N and C_1. For example, while C_1 (inverse of the MOI) varies two orders of magnitude over the range of the molecules presented in Table I, the ratio $N\Delta C_1/C_1$ remains practically constant. Below, we discuss the experimental systematics for each ratio and contrast them with the O(4) predictions.

(a) $\Delta E/NC_1$: ΔE and C_1 are the two most important spectroscopic quantities characterizing the vibrational and rotational excitations, respectively. When $\kappa'=0$, the O(4) limit has the parameter-free prediction of 4 for this ratio, which is smaller than the observed values listed in Table I. The halides are the closest to the O(4) value with some 10–30 % deviation, but as one moves to heavier and more symmetric molecules, the difference becomes a factor of 2–3. Clearly one needs a smaller C_1 (larger MOI) than predicted by the O(4) limit. An easy way to achieve this is to introduce

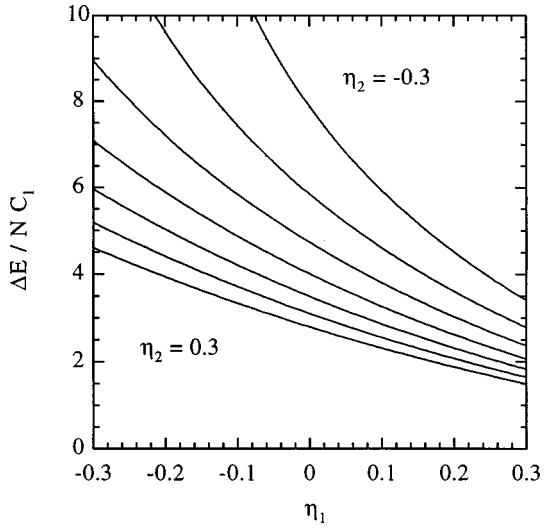

FIG. 1. The effect of the one- and two-body symmetry-breaking terms with strength parameters η_1 and η_2 on the ratio $\Delta E/NC_1$. The parameter η_2 is varied from -0.3 to 0.3 in steps of 0.1.

the $\hat{L}\cdot\hat{L}$ term in the Hamiltonian with a negative κ'. But as stressed earlier, this is an artificial way to increase the MOI because it does not lead to a corresponding increase in molecular size. A better and physically more appealing way would be to break the O(4) limit in such a way that the size parameter r (or a) gets larger than the O(4) value of 1 as the MOI increases.

(b) N^2C_2/C_1: This ratio measures the softness of a rotor, that is, the ability of a molecule to stretch while it rotates faster and faster in the ground band. The experimental values in Table I cover a wide range, from -0.2 in the halides to -0.02 in AlS. It vanishes in the O(4) limit, which corresponds to a rigid rotor. But as seen in Sec. III, any breaking of the O(4) limit leads to nonzero values for this ratio, and hence they could provide a more natural explanation for the softness parameter than including the term $(\hat{L}\cdot\hat{L})^2$ in the Hamiltonian.

(c) N^4C_3/C_1: This ratio provides a correction to the softness at high spins, and it is usually positive. Again it vanishes in the O(4) limit. One can accommodate the experimental values by either breaking the O(4) limit or including $(\hat{L}\cdot\hat{L})^3$ term in the Hamiltonian.

(d) $N\Delta C_1/C_1$: The differential change in C_1 as depicted by this ratio remains remarkably constant for the diatomic molecules listed in Table I. The negative sign reflects the fact that the MOI of the molecules gets larger with increasing vibrational number. In the O(4) limit, all the bands have the same MOI, and hence this ratio vanishes. The observed changes in the MOI can be reproduced by either including the quartic term $\hat{D}\cdot\hat{D}\ \hat{L}\cdot\hat{L}$ in the Hamiltonian or, more generally, by breaking the O(4) limit.

(e) $N\Delta C_2/C_2$: This is similar to (d) above but for the softness parameter C_2. The experimental values show more variation but are generally negative (except AlO). It is indeterminate in the O(4) limit as $C_2=0$ for all bands.

As stressed earlier, the change in band structure is linear (to leading order) for low-lying bands; therefore the above quantities provide a good overall representation for the spectroscopic data.

A. Minimal breaking of O(4)

We first consider a minimal breaking of the O(4) limit via the Hamiltonian (2.3). The effect of the $\hat{n}_p$ and $\hat{n}_p^2$ terms on the ratios (a)–(e) introduced above are shown in Figs. 1–3. In each figure, a particular ratio is plotted against the parameter η_1 for various values of η_2. Both parameters are varied in the range of $[-0.3,0.3]$, η_1 continuously and η_2 in steps of 0.1. In Fig. 1, we show the effect of the symmetry breaking on the ratio $\Delta E/NC_1$, which is seen to be coherent for η_1 and η_2. That is, they both reduce this ratio from its O(4) value of 4 for positive values and, conversely, increase it for negative values. The latter range is preferred by the experimental values quoted in Table I, which require a larger MOI than that provided by the dipole interaction alone. Note that for negative η_1 or η_2, a (or r) gets larger than the O(4) value [see Eq. (3.37)]. Thus the increase in the MOI is associated with a corresponding increase in molecular size. We remark that the situation in the IBM description of deformed nuclei is exactly the opposite; namely, the dominant quadrupole-quadrupole interaction there leads to a too large MOI that needs to be reduced by the addition of (positive) one-body energies [24]. This choice of sign in the IBM has firm microscopic foundations in the pairing property of the nucleon-nucleon interaction. In the case of diatomic molecules, there is no microscopic basis for the bosons, and the

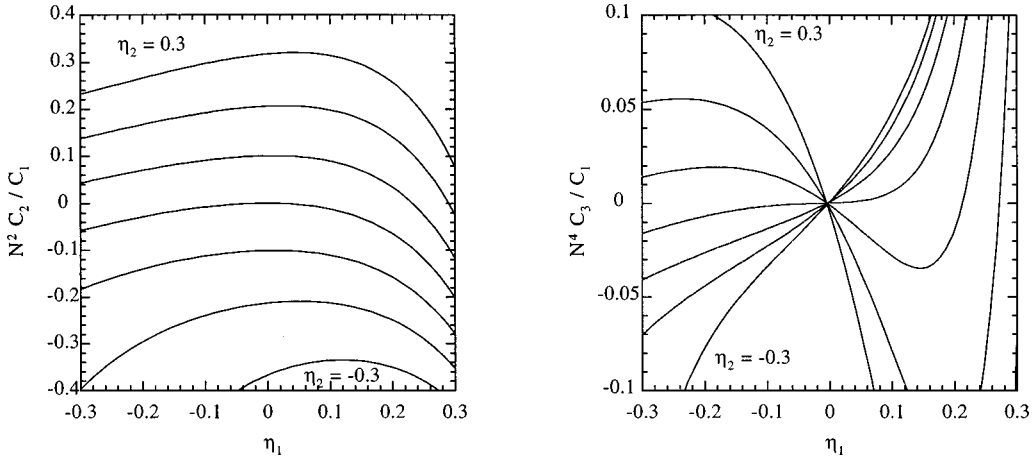

FIG. 2. Same as Fig. 1 but for the ratios N^2C_2/C_1 and N^4C_3/C_1.

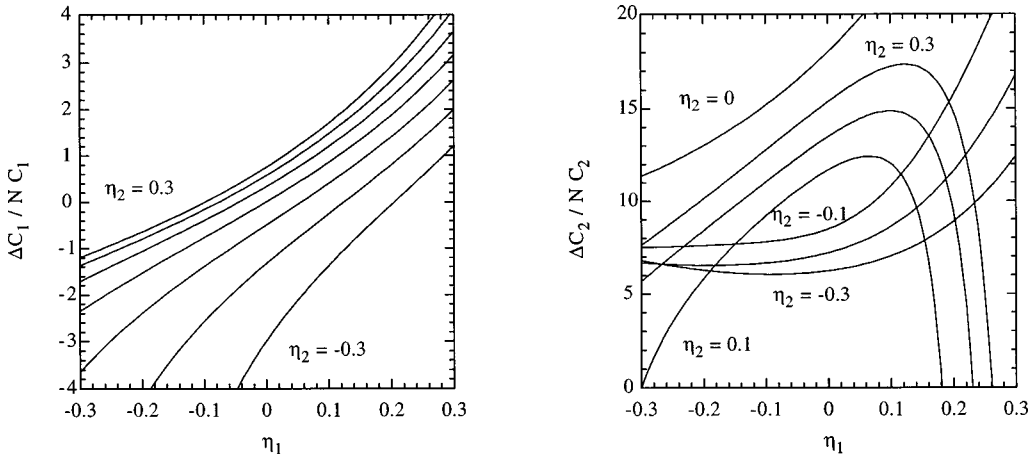

FIG. 3. Same as Fig. 1 but for the ratios $N\Delta C_1/C_1$ and $N\Delta C_2/C_2$.

choice of sign for the symmetry-breaking terms is purely motivated by phenomenology.

In Fig. 2, we study the variation of the ground-band MOI with spin. The two ratios N^2C_2/C_1 and N^4C_3/C_1, which measure the deviation from the rigid-rotor behavior, are plotted in Figs. 2(a) and 2(b), respectively. Symmetry breaking by η_1 gives the correct sign for N^2C_2/C_1 but the magnitude is not large enough to accommodate the observed values, especially for the halides. The positive range of η_2 leads to the wrong sign; thus they are excluded by this set of data. The negative range of η_2, on the other hand, gives the correct sign and they are much more effective than η_1 in reproducing the experimental range. The ratio N^4C_3/C_1 has the wrong sign in most cases when both η_1 and η_2 are negative. Nevertheless, a small positive η_1 and a larger negative η_2 could still explain all three ratios discussed so far.

The change in the MOI among different bands is illustrated in Fig. 3. The ratios $N\Delta C_1/C_1$ and $N\Delta C_2/C_2$ are plotted in Figs. 3(a) and 3(b), respectively. The former can be described by a band value satisfying $\eta_1+\eta_2\approx-0.2$, which is still consistent with the previous ratios. But the latter ratio, which is indeterminate in the O(4) limit, exhibits large variations far outside the experimental range for any value of the symmetry-breaking terms. Explanation of this ratio calls for higher-order terms in the Hamiltonian.

As already mentioned in Sec. IV, the one-body dipole operator is not sufficient to describe the infrared transitions beyond $\Delta v=1$. Here we discuss the case of $\Delta v=1$ dipole transitions, where symmetry breaking provides the right order of magnitude as far as the N dependence is concerned. From Eqs. (4.6) and (4.4) the ratio of a $1\rightarrow0$ to $0\rightarrow0$ transition is roughly given by $\eta_1/\sqrt{N}$. Since the dynamic considerations above limit the values η to about 0.2, symmetry breaking could provide only a fraction of the experimental ratio. This again underscores the importance of higher-order terms in the transition operator.

B. Higher-order terms

Here we discuss the symmetry breaking due to the higher-order terms, namely, three-body interactions in the Hamiltonian and two-body terms in the dipole transition operator. The effect of the three cubic terms on the ratios (a)–(e) are shown in Figs. 4–8. The presentation is similar to Figs. 1–3 with η_2 being replaced by η_3 in (a), η_3' in (b), and η_3'' in (c) of each figure. The effect of the cubic terms on the ratio $\Delta E/NC_1$ is shown in Fig. 4. The curves in Fig. 4 exhibit broadly similar features as in the case of η_2 in Fig. 1; thus

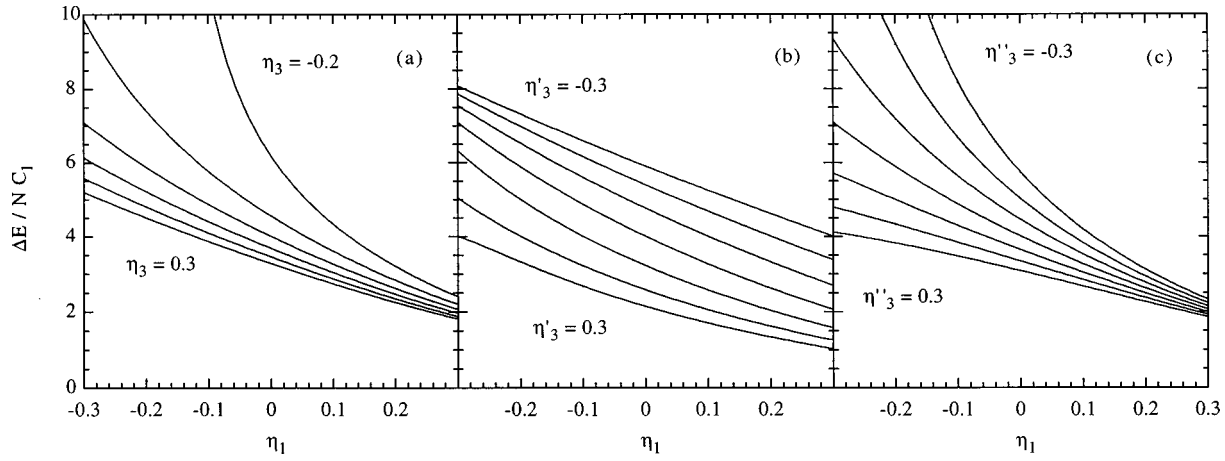

FIG. 4. The effect of the cubic terms with strength parameters η_3, η_3', and η_3'' on the ratio $\Delta E/NC_1$. The parameters are varied from -0.3 to 0.3 in steps of 0.1, except for η_3 which is varied from -0.1 to 0.3. Lower η_3 values are excluded because they lead to excessive fluctuations in the graphs.

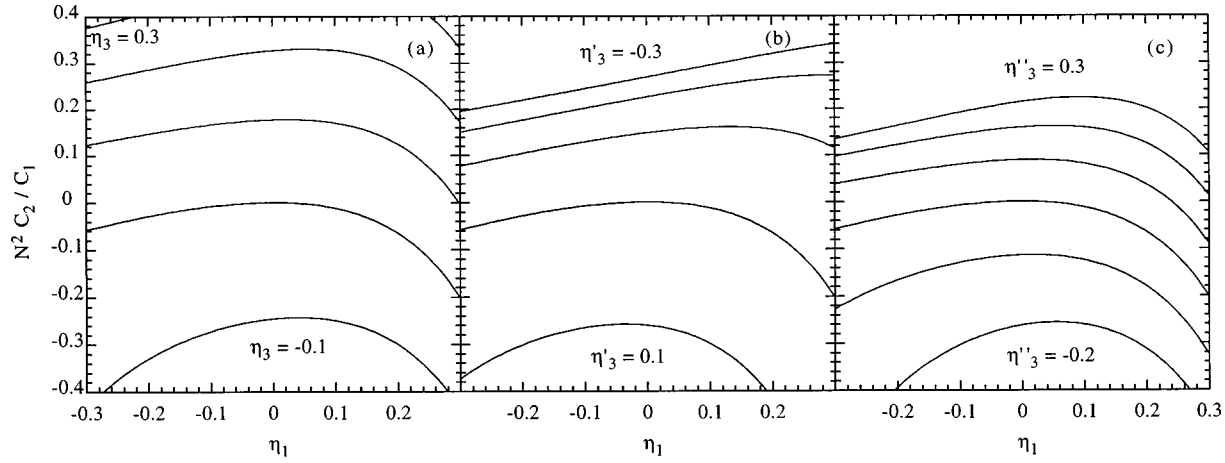

FIG. 5. Same as Fig. 4 but for the ratio N^2C_2/C_1.

the same comments apply here. In details, the η_3' dependence is more uniform and weaker compared to the others.

In Fig. 5, we study the dependence of the ratio N^2C_2/C_1 on the cubic terms. Again, the curves in Fig. 5 exhibit similar patterns as in Fig. 2(a) showing the η_2 dependence. Two important differences are that η_3 is even more effective than η_2 in inducing changes in this ratio, and the sign dependence for η_3' is reversed compared to the others. These features would be helpful in a fine-tuning of the parameters. In Fig. 6, we repeat the same study for the ratio N^4C_3/C_1. In this case, there are no common features among different figures. Noteworthy is the η_3 dependence, which is very sensitive to this ratio, and hence η_3 would be best determined by fits to the C_3 coefficient of the ground-band MOI.

The variation in MOI with bands is studied in Figs. 7 and 8. In Fig. 7, the dependence of the ratio $N\Delta C_1/C_1$ on the cubic terms is seen to be similar to that of η_2 in Fig. 3(a), but much weaker in its effect. Thus this ratio should be fitted by the η_1 and η_2 parameters. The unstable nature of the ratio $N\Delta C_2/C_2$ encountered in Fig. 3(b) is cured by the addition of the cubic terms (Fig. 8). The η_3 range is still outside the experimental range but the other two could explain the data. Clearly, in order to reproduce this ratio, one has to balance the cubic parameters carefully.

Inclusion of the two-body term in the dipole operator clearly cures the problem in the $\Delta v=1$ transitions mentioned above. From Eqs. (4.9) and (4.8), the $1\rightarrow 0/0\rightarrow 0$ ratio is given by $1/\sqrt{N}$, consistent with the data. However, the same ratio for the $\Delta v=2$ transition is still proportional to η; hence it suffers from the same problem. This again can be resolved by either including the three-body term in Eq. (2.5) or, more practically, using the exponential form (2.6).

VI. CONCLUSIONS

In this article, we have developed analytic $1/N$ expansion solutions for the vibron model of diatomic molecules and used the results in a systematic study of symmetry-breaking effects in energy levels and electric transitions among them. We have shown that the O(4) results can be improved by including symmetry-breaking terms in the Hamiltonian. Symmetry breaking could offer a more economical and physical description of spectroscopic data compared to the symmetry-preserving approach, and should be considered in detailed studies in the future.

A unique aspect of the formalism that is worthwhile emphasizing is that the solutions obtained for the ground-band energies and transitions are exact for arbitrary Hamiltonians and parameters. For the vibrational bands, the ansatz (2.33), generalized from the O(4) wave functions, reproduces the numerical diagonalization results for the energies and in-band transitions, but leads to small discrepancies in spin-

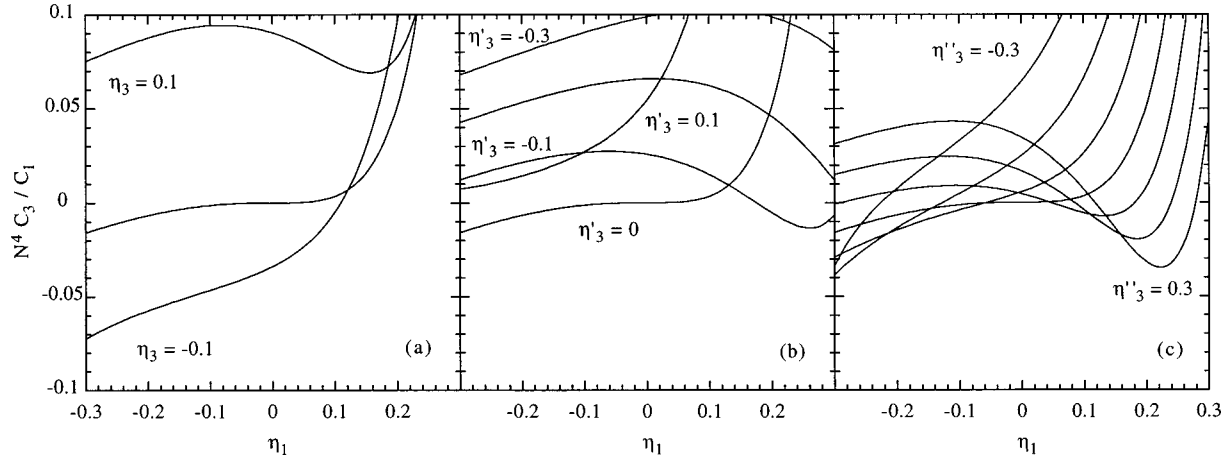

FIG. 6. Same as Fig. 4 but for the ratio N^4C_3/C_1.

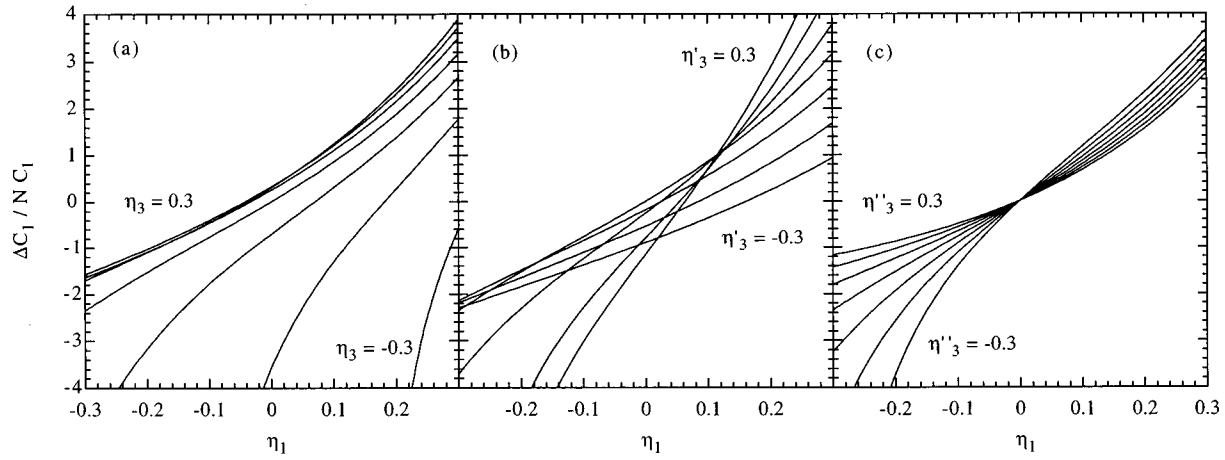

FIG. 7. Same as Fig. 4 but for the ratio $N\Delta C_1/C_1$.

dependent terms of interband transitions. While this has no practical consequences, it suggests that the vibrational bands are likely to have more complicated forms in the intrinsic frame than given in Eq. (2.33).

The simplicity of the vibron model also allowed us to go beyond the usual boundaries of the IBM, and explore, for example, the effects many-body terms in the Hamiltonian and transition operators, as well as multiphonon bands. Since the formalism in both models is very similar, one could extract lessons for the IBM from the present results. The variation of the MOI with bands provides a relevant example. In both collective nuclei and molecules, the MOI of $K=0$ bands gets larger with increasing phonon number. Reproducing this feature in the IBM has been an outstanding problem [25]. Inspection of Fig. 3(a) shows that the positive one-body term $\hat{n}_d$ could be the source of the problem, and an attractive two-body term $\hat{n}_d^2$ is needed to compensate for it and to make the MOI in the β band larger.

Finally, the formalism for the U(4) SGA provides the basis for extension of the $1/N$ expansion technique to polyatomic molecules, which will be pursued in future articles.

ACKNOWLEDGMENT

This research was supported in part by the Australian Research Council.

APPENDIX A: NORMALIZATION COEFFICIENTS

Below, we tabulate the coefficients α_{nm} in Eq. (2.32) up to the order $1/N^6$ in a layer format. Layers are defined such that α_{nm} with $n-m+1=k$ belongs to the kth layer; that is, α_{nn} forms the first layer, α_{nn-1} second, etc.:

first layer: $\alpha_{nn}=1;$

second layer: $\alpha_{10}=a, \quad \alpha_{21}=6a-2, \quad \alpha_{32}=18a-8,$

$\alpha_{43}=20(2a-1), \quad \alpha_{54}=75a-40,$

$\alpha_{65}=14(9a-5);$

third layer: $\alpha_{20}=2a^2, \quad \alpha_{31}=6(7a^2-6a+2),$

$\alpha_{42}=4(75a^2-80a+27),$

$\alpha_{53}=4(325a^2-375a+127),$

$\alpha_{64}=28(150a^2-180a+61);$

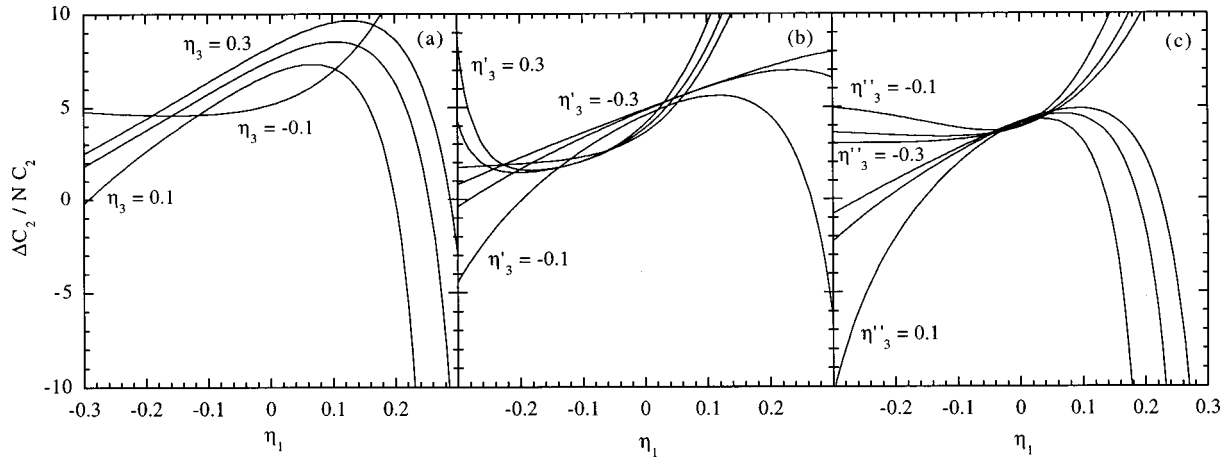

FIG. 8. Same as Fig. 4 but for the ratio $N\Delta C_2/C_2$. The curves for $\eta_3=0$, $\eta'_3=0$, and $\eta''_3=0$ lie outside the figures [cf. Fig. 3(b)].

fourth layer: $\alpha_{30}=6a^3$,

$\alpha_{41}=24(15a^3-25a^2+20a-6)$,

$\alpha_{52}=4(1350a^3-2600a^2+2025a-576)$,

$\alpha_{63}=24(1750a^3-3500a^2+2667a-731)$;

fifth layer: $\alpha_{40}=24a^4$,

$\alpha_{51}=120(31a^4-90a^3+130a^2-90a+24)$,

$\alpha_{62}=24(4515a^4-14000a^3+18900a^2-12096a+3000)$;

sixth layer: $\alpha_{50}=120a^5$,

$\alpha_{61}=720(63a^5-301a^4+700a^3-840a^2+504a-120)$. (A1)

Normalizations for the vibrational bands have exactly the same form as Eq. (2.32) but the coefficients α_{nm} have different values. The exception is the first-layer coefficients which remain the same, i.e., $\alpha_{nn}=1$. For the $v=1$ band, the second- and third-layer coefficients are given by

second layer: $\alpha_{10}=2a-4$,

$\alpha_{21}=8a-14$,

$\alpha_{32}=21a-32$,

$\alpha_{43}=44a-60$,

$\alpha_{54}=20(4a-5)$,

$\alpha_{65}=132a-154$;

third layer: $\alpha_{20}=6(a^2-4a+4)$,

$\alpha_{31}=18(5a^2-17a+14)$,

$\alpha_{42}=4(114a^2-352a+263)$,

$\alpha_{53}=4(470a^2-1330a+907)$

$\alpha_{64}=4(1200a^2-3090a+1957)$. (A2)

For the $v=2$ band, the same coefficients to power $1/N^4$ are

second layer: $\alpha_{10}=3a-8$,

$\alpha_{21}=2(5a-13)$,

$\alpha_{32}=8(3a-7)$,

$\alpha_{43}=4(12a-25)$;

third layer: $\alpha_{20}=2(5a^2-32a+48)$,

$\alpha_{31}=6(23a^2-108a+130)$,

$\alpha_{42}=4(153a^2-672a+739)$. (A3)

APPENDIX B: O(4) RESULTS

The O(4) limit of the vibron model has been solved exactly using group theoretical techniques [2,3]. Since it provides a valuable reference point in both formulation of the 1/N expansion and checking the accuracy of the analytical formulas, we collect here some of the relevant results. The O(4) Casimir operator and its expectation value in a state $|N,v,L\rangle$ are given by

$$\hat{C}_2(O(4))=\hat{D}\cdot\hat{D}+\hat{L}\cdot\hat{L},$$

$$\langle N,v,L|\hat{C}_2(O(4))|N,v,L\rangle=N(N+2)-4(N+1)v+4v^2. \quad \text{(B1)}$$

Thus the energy eigenvalues of the O(4) Hamiltonian (2.1) are

$$\langle N,v,L|\hat{H}_{\mathrm{O}(4)}|N,v,L\rangle=-\kappa[N(N+2)-4(N+1)v+4v^2]+(\kappa+\kappa')\overline{L}. \quad \text{(B2)}$$

Explicit expressions for the O(4) wave functions, both in coordinate space and second-quantized form, are available in the literature [3]. Here we quote a particularly useful recursion relation that allows construction of the vibrational bands from the ground band of systems with lower boson number,

$$|N,v,L\rangle=\mathcal{C}_{Nv}(s^\dagger s^\dagger-\vec{p}^\dagger\cdot\vec{p}^\dagger)^v|N-2v,0,L\rangle, \quad \text{(B3)}$$

where $\mathcal{C}_{Nv}$ is a normalization factor:

$$\mathcal{C}_{Nv}=(-2)^{-v}\left[\frac{(N-2v+1)!}{v!(N-v+1)!}\right]^{1/2}. \quad \text{(B4)}$$

Rewriting the ground-band state as a projection from the condensate $|N-2v,0,L\rangle\propto P^L_{00}|N-2v,0\rangle$, and noting that the projection operator commutes with the scalar operator $(s^\dagger s^\dagger-\vec{p}^\dagger\cdot\vec{p}^\dagger)$, it is clear that intrinsic states have the same form as in Eq. (B3):

$$|N,v\rangle=\mathcal{C}_{Nv}(s^\dagger s^\dagger-\vec{p}^\dagger\cdot\vec{p}^\dagger)^v|N-2v,0\rangle. \quad \text{(B5)}$$

In terms of the intrinsic boson operators $b=(s+p_0)/\sqrt{2}$, $b'=(s-p_0)/\sqrt{2}$, the vibrational bands in Eq. (B5) can be written as

$$|N,v\rangle=2^v\mathcal{C}_{Nv}[(N-2v)!]^{-1/2}\times[b^\dagger b'^\dagger+p_1^\dagger p_{-1}^\dagger]^v(b^\dagger)^{N-2v}|0\rangle. \quad \text{(B6)}$$

Matrix elements of various operators have been calculated in the O(4) limit [2,3]. Here we quote a few of them that are used in checking the 1/N expansion results:

$$\langle N,v,L|\hat{n}_p|N,v,L\rangle = \frac{N-1}{2} + \frac{(N+2)\overline{L}}{2(N-2v)(N-2v+2)}, \tag{B7}$$

$$\langle N,v,L+1|\hat{D}|N,v,L\rangle = [(L+1)(N-2v+L+2)(N-2v-L)]^{1/2}. \tag{B8}$$

APPENDIX C: ANGULAR MOMENTUM SUMS

In evaluating matrix elements, one often needs to couple the d functions with Clebsch-Gordan coefficients using

$$d^L_{mn} d^{L'}_{m'n'} = \sum_J \langle LmL'm'|J\mu\rangle \langle LnL'n'|J\mu'\rangle d^J_{\mu\mu'}. \tag{C1}$$

After the angular integration, Eq. (C1) leads to angular momentum sums with the d function replaced by powers of $\overline{J}$. These sums can be evaluated using the techniques described in Appendix B of Ref. [4]. Here we quote the results for the case $m=m'=n=n'=0$, which are encountered most in this paper:

$$S_n = \sum_J \langle L0L'0|J0\rangle^2 \overline{J}^n. \tag{C2}$$

The first few of the sums are given by

$$S_0 = 1, \quad S_1 = \overline{L} + \overline{L'}, \quad S_2 = \overline{L^2} + 4\overline{LL'} + \overline{L'^2},$$

$$S_3 = \overline{L^3} + \overline{LL'}(9\overline{L} + 9\overline{L'} - 4) + \overline{L'^3},$$

$$S_4 = \overline{L^4} + 4\overline{LL'}[4\overline{L^2} + 9\overline{LL'} + 4\overline{L'^2} - 5(\overline{L} + \overline{L'}) + 4] + \overline{L'^4}. \tag{C3}$$

[1] F. Iachello and A. Arima, *The Interacting Boson Model* (Cambridge University Press, Cambridge, England, 1987).
[2] F. Iachello and R.D. Levine, *Algebraic Theory of Molecules* (Oxford University Press, Oxford, 1995).
[3] A. Frank and P. Van Isacker, *Algebraic Methods in Molecular and Nuclear Structure Physics* (Wiley, New York, 1994).
[4] S. Kuyucak and I. Morrison, Ann. Phys. (N.Y.) **181**, 79 (1988); **195**, 126 (1989).
[5] S. Kuyucak, in *Perspectives for the Interacting Boson Model*, edited by R.F. Casten *et al.* (World Scientific, Singapore, 1994), p. 143.
[6] H.J. Lipkin, N. Meshkov, and A.J. Glick, Nucl. Phys. **62**, 188 (1965).
[7] S. Kuyucak and M.K. Roberts, Chem. Phys. Lett. **238**, 371 (1995).
[8] F. Iachello, A. Leviatan, and A. Mengoni, J. Chem. Phys. **95**, 1449 (1991).
[9] A. Leviatan and M. Kirson, Ann. Phys. (N.Y.) **188**, 142 (1988).
[10] O.S. Van Roosmalen and A.E.L. Dieperink, Ann. Phys. (N.Y.) **139**, 198 (1982).
[11] S. Levit and U. Smilansky, Nucl. Phys. A **389**, 56 (1982).
[12] O.S. Van Roosmalen, R.D. Levine, and A.E.L. Dieperink, Chem. Phys. Lett. **101**, 512 (1983).
[13] O.S. Van Roosmalen, I. Benjamin, and R.D. Levine, J. Chem. Phys. **81**, 5986 (1984).
[14] B. Shao, N.R. Walet, and R.D. Amado, Phys. Rev. A **46**, 4037 (1992); **47**, 2064 (1993).
[15] A. Mengoni and T. Shirai, Phys. Rev. A **50**, 863 (1994).
[16] P. Ring and P. Schuk, *The Many-Body Problem* (Springer-Verlag, New York, 1980).
[17] D.M. Brink and G.R. Satchler, *Angular Momentum* (Oxford University Press, Oxford, 1968).
[18] J. Schwinger, in *Quantum Theory of Angular Momentum*, edited by L.C. Biedenharn and H. van Dam (Academic Press, New York, 1965), p. 350.
[19] S. Kuyucak and K. Unnikrishnan, J. Phys. A **28**, 2101 (1995).
[20] A.F. Diallo, E.D. Davies, and B.R. Barrett, Ann. Phys. (N.Y.) **222**, 159 (1993).
[21] S. Wolfram, MATHEMATICA (Addison-Wesley, Redwood City, CA, 1991).
[22] S. Kuyucak and I. Morrison, Phys. Rev. Lett. **62**, 1029 (1989).
[23] K.P. Huber and G. Herzberg, *Molecular Spectra and Molecular Structure IV: Constants of Diatomic Molecules* (Van Nostrand, New York, 1979).
[24] S. Kuyucak and S.C. Li, Phys. Lett. B **354**, 189 (1995).
[25] S. Kuyucak and I. Morrison, Phys. Rev. C **38**, 2482 (1988).